Electrochemical CO_2 reduction and the path towards Industrialisation

PTFE-based modification on carbon GDLs to enable acidic CO_2 reduction towards C2+ products.

Thesis - Energy, Flow and Process Technology

Thomas Meyer Ranneft

Delft University of Technology

TU Delft

Electrochemical CO_2 reduction and the path towards Industrialisation

PTFE-based modification on carbon GDLs to enable acidic CO_2 reduction towards C2+ products.

by

Thomas Meyer Ranneft

Thomas Meyer Ranneft 4597753

TU Delft Instructor:	Dr. R. Kortlever
TU delft supervisor:	Postdoctoral researcher Dr. Ahmed Mohsen Mohamed
SCW Instructor:	Dr. Maxim Ariëns & Hidde Rommens
Thesis committee:	Dr. R. Kortlever, Dr. A. M. Mohamed, Dr. M. Ariens Prof. Dr. Ir. W. De Jong, Dr. T.E. Burdyny
Project Duration:	Sept., 2023 - Okt., 2024
Faculty:	Faculty of Process and Energy, Delft

TU Delft

Abstract

While the potential of CO_2R towards C2+ products is widely recognised, the technique struggles with industrial scale-up. Within this report, an elaborated analysis is performed on the industrial potential of CO2 reduction, more specifically on cells operating in a strongly acidic medium. These type of cells boast not only a high CO2 conversion of over 70% but also potentially enable the extraction of liquids at concentrations required for efficient separation as opposed to anion exchange membrane (AEM) based cells. Although immature the acidic cell has been proven to achieve excellent C2+ product formation with a faradaic efficiency above 75%. A currently not surpassed barrier is the scale-up of acidic cells above 1 cm^2 as most utilize a non-conductive polytetrafluoroethylene (PTFE) membrane. Within this research an alternate approach was examined adopting the conductivity of a modified commercial carbon gas diffusion layer (GDL). Using the hydrophobicity of PTFE beneath, within and on top of the catalyst layer, a CO_R promoting environment is created. Within this research, one of the largest highly acidic (pH<1) cells to date has been devised while yielding a respectable faradaic efficiency towards C2+ products of 53%.

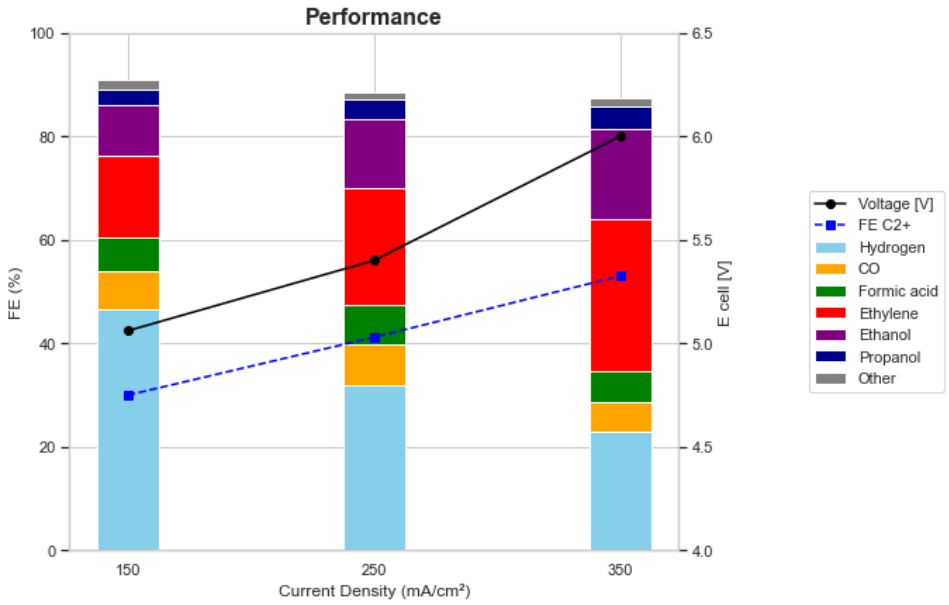

Figure 1: Influence of the current density on CO_2 reduction efficiency and product selectivity. Faradaic efficiency of the generated products at three different current densities with a feed rate of CO_2 of 15 sccm, 1 M H_3PO_4/KCl catholyte and 1 M H_3PO_4 anolyte. Performance after 40 minutes of electrolysis

Contents

1

Introduction

Amidst the ongoing energy transition carbon capture is gaining more momentum. The reduction of fossil fuel use is happening at a slower rate then was hoped for and it is getting more clear by the day that carbon capture and specifically carbon capture and utilisation will play a vital role in the mitigation of climate change. One promising approach in this context is the electrochemical reduction of carbon dioxide (CO_2R). Although this technology is still in its early stages, there is growing excitement about its potential for large-scale use in industries. Currently problems within CO_2 reduction include low long-term stability, low CO_2 utilization, however a large variety of cells, each with different characteristics, signify an incredible potential. This article aims to examine the electrochemical process and provide a detailed exploration of the possibilities and limitations of each type. Beyond that, this report will evaluate different configurations and design a cell with the specific aim of enabling industrialisation.

2

Background information

2.1. Aim of the project

CO_2R is an upcoming immature technology with an incredible potential, with the ability of producing high value compounds such as carbon monoxide, ethylene, ethanol and propanol. Currently a number of key problems obstruct the step towards industrialization such as CO_2 conversion rate, long term stability and product extraction. This report specifically focuses on liquid products, which are valuable and easily transportable worldwide The following research question will be assessed in the literary review of this report. Based on these question and its sub-questions an elaborate assessment will be made on the potential for industrialization of various cell architectures with the aim on liquid products.

What is the optimal configuration in terms of electrode, catalyst and electrolyte for direct CO_2 electrolysis towards high energy density liquids with minimal downstream process?

This research question is evaluated along the following two sub-questions.

- What is the performance of current state of the art CO_2 electrolysers towards liquid products, and what liquid product is currently the most optimal goal product?
- What are the design distinct downstream processes associated with CO_2R towards liquid products?

The first question is a survey of the current state of technology, meant to explore different design options and orientate on the subject. The second question will explore the difficulties currently present within scaling up on an industrial level. The main cost drivers are determined resulting in a trade-off of different designs minimising these industrial processes. Along with the last driving question an optimal design is determined and a cell type specified. This cell will be researched and produced throughout the experimental part of the report.

2.2. Electrochemical cells and their working principle

Electrochemical cells come in all shapes and sizes, within the following section different types of cells will be introduced and their working principle will be explained. This section functions to introduce 4 different cell types and to provide a first insight into the mechanism behind electrochemistry.

2.2.1. Cell types

An electrochemical cell consists of multiple distinct components as depicted graphically in Figure 2.1 below. In this paragraph, the working principle of an electrochemical cell will be explained shortly and in plain english.

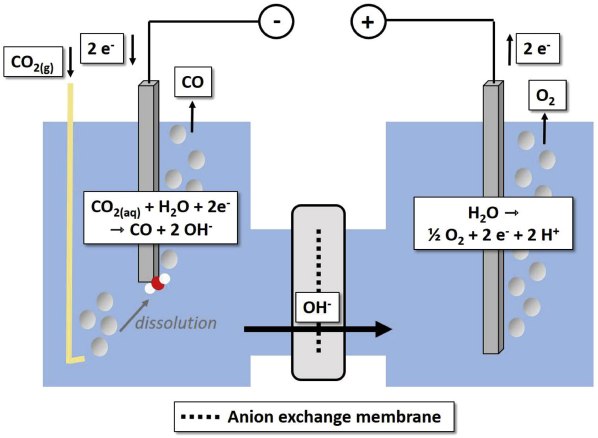

Figure 2.1: Schematic of a CO_2R electrolytic cell, note that this is an H-cell for explanatory purposes. [14].

In the case of this report, the electrochemical cell is called an electrolytic cell as a voltage is applied to drive a non-spontaneous reaction of producing (liquid) C-products and oxygen from CO_2 and H_2O respectively. On the right side of the cell, at the anodic electrode or anode, electrons are produced via the Oxygen Evolution Reaction (OER) along with consumption of the reactant H_2O. On the left side, at the cathodic electrode or cathode, electrons are consumed via CO_2R along with consumption of the reactant CO_2. The electrodes are externally connected electrically, within the cell an electrolyte provides conductance. A voltage is applied on the electrodes and in order to close the electric circuit an ionic current, charged ions migrating from one electrode to the other fulfilling a role analogous of electrons within an electric current, is induced through the electrolytes. The electrolyte on the cathode side is called the catholyte while the electrolyte on the anode side is called the anolyte.
Chemical reactions must be present as these are necessary to sustain the ionic current and produce ions of similar charge. The electrodes are separated by a selective membrane to prevent products of one electrode to be reacted away on the other electrode [14].

The H-cell is the simplest of cell configurations within electrochemistry and is depicted . It consists of two chambers filled with stationary water or electrolyte and an electrode, the chambers are separated by either a membrane, diaphragm or a salt-bridge enabling ion migration between the above mentioned chambers while limiting diffusion of reaction products. In the figure presented Figure 2.1 a reference electrode is included, this reference electrode measures potential on the electrode in the half-cell considered, the working electrode.

Due to the simplistic and controllable design of an H-cell, experimental and fundamental research is often conducted using H-cells. As described in [1] and [38], the H-cell is among other topics often used in the evaluation of catalytic materials, for example their interactions and efficiencies, and product cross-over. Current densities of other type of cells are generally higher due to high ionic resistance and low mass-transport properties of the H-cell. Therefore, H-cells will not be taken into account while performing the design trade-offs considering configuration.

Another type of cell are solid oxide electrochemical cells. SOEC's distinguish themselves by their operation at elevated temperatures above 600°C and the solid electrolyte separating the electrodes allowing only protons or oxygen to protrude. Although praised for its high efficiency and high current density SOEC's, complex electrochemistry, susceptibility to impurities within the feed stream and their inclination towards production of CO exclude SOEC from this research [38] [5].

Microfluidic cells are a relatively novel type of electrochemical cell and is distinctive in its lack of a membrane. The cathode and anode are separated solely by diffusive properties within a thin layer (<1 mm) of electrolyte [1]. Microfluidic cells and their design enable rapid testing of various catalysts under different conditions and are suitable for testing both GDE's and catalyst layer performances [38]. However, microfluidic cells are not solely applicable to experimental research, multiple articles have reported microfluidic cells with high current density and faradaic efficiency (FE). Nevertheless, these type of cells will not be taken into account as they are complex to scale-up and direct circulation of electrolyte, necessary for increasing the ethanol content before distillation, is deemed impossible [14].

The last type of cell to be presented are flow cells, boasting a similar working principle as H-cells with the key difference of a flowing electrolyte. This allows for continuous production and extraction of target compounds, a necessary trade towards commercialization of CO_2 reduction cells [33]. This research shall focus on the design of such flow cells.

2.3. Target product selection

In order to understand the electrochemical cell reducing carbon dioxide the first steps is to understand what kind of reactions occur at the anode and the cathode. Therefore this chapter starts with an overview of generally found compounds and the current state of technology, additionally the target product is determined.

2.3.1. Product overview

Dependent on a combination of factors such as temperature, pressure, pH and catalyst, a variety of products containing carbon could be created by use of an electrochemical cell. A summarized overview of CO_2R reaction paths and overall reactions are found within Figure A.3 and Figure A.2.
Within the scope of this research 2 specific requirements on the total product mix are as presented.

1. Liquid component of product mix should have a higher heating value (HHV) of at least 20 [MJ/kg].
2. Liquid component of product mix should be soluble in water with a solubility rate of at least 40wt%.

It should be noted that as these requirements address the product mix, they do not imply boundaries on individual liquid components produced. The message to take away is that all gasses within the product mix will are undesirable and production should be minimized. The second requirement is satisfied for all potential liquid products.

The primary compounds found in literature to be produced are summarized in Table 2.1 [1][16][18]. Furthermore, the following liquid products mentioned in the sources cited were found to be insignificant due to the small quantities of production; Allyl alcohol, Formaldehyde, Acetaldehyde, Oxalic acid, Ethylene glycol, Glycolic acid, Acetone, hydroxyacetone and Propionaldehyde.

Name	Chemical form.	Phase[1]	HHV [MJ/kg]	Remarks
Carbonmonoxide	CO	Gas	10,1	Gas
Methanol	CH_3OH	Liq.	23	Diff. to produce
Methane	CH_4	Gas	55,5	Gas
Formic acid	HCOOH	Liq.	5,51	Low HHV
Ethylene	C_2H_4	Gas	50,3	Gas
Ethanol	C_2H_5OH	Liq.	29,7	-
Ethane	C_2H_6	Gas	51,9	Gas
Acetic acid	CH_3COOH	Liq.	15,6	Diff. to produce
n-Propanol	C_3H_7OH	Liq.	33,6	In comb. with EtOH

Table 2.1: Product variety found in literature;
1: 298K 1 atm.

Based upon the table a conclusion could be drawn on the determination of the goal product of this report. The first and most obvious filter applied is based on phase of the compound at 25°C as the product needs to be a liquid. A second evident filter is based on the higher heating value of the product, as stated before an as high as possible HHV is desired, formic acid is excluded. Lastly, the products are filtered based on ease of production as reported in literature, this filter excludes products which are as of now at low technical maturity, methanol and acetic acid.

Direct production of Acetic acid is found to be in minor quantities [62]. One report showed both high FE (70%) and partial current density (425 mA/cm^2) in electrochemical reduction of CO towards acetic acid [32]. However, upon inspection it is a questionable result as anodic oxidation of ethanol towards acetic was not accounted for, a phenomenon that could be observed in anion exchange membrane

based cells [30]. As only little sources were found reporting a current density above 100 mA/cm^2 and the specific energy of acetic acid is relatively low, it was deemed too big of a risk to focus on acetic acid specifically and the compound has been discarded as aimed upon product.

Methanol is deemed to be difficult to produce as only a single report could be found to have reached a partial current density above 100 mA/cm^2 within multiple reviews [18][39][65][68], this current density has been achieved in an H-cell. Electrochemical cells with the aim to produce methanol are therefore disregarded in the remaining of this report.

After review of literature as presented in Table A.2 it can be concluded that ethanol is a promising compound within the broad objective of producing liquid hydrocarbons by electrochemistry, ethanol production shall therefore be the aim of this report.

Within Table A.2 a highlighted set of electrochemical cells is presented, these are the most relevant results found throughout the literature study based on a minimum stability of 2 hours and a current density of at least 100 mA/cm^2. Note that only flow cells have been taken into account as H-cells are not industrially relevant. A general profile has been deduced and is shown in Table 2.2 Note that biases are inevitable as this is a small sample.

$J_{liq.}$ [mA/cm^2]	**V_{cell}**	**Stab. [h]**	**CO_2 conv. [%]**	**$EE_{liq.}$ [%]**	**FE [%]**			
					H2	**C2**	**EtOH**	**Liq.**
120-300	3.5-5	5-35	5-30*	10-25	5-20	50-90	20-50	30-60

Table 2.2: General profile ethanol producing electrochemical cells, *Wide variety in value dependent on cell type

Considering current density, voltage and stability, the minimum and the maximum are defined by taking one standard deviation from the average. Considering the conversion of CO_2, the total conversion rate is presented, in other words 5-30 % of CO_2 entering the cell will be converted. The faradaic efficiencies have been based upon the cells examined. Note that the current density only comprises the partial current density towards alcohols and acetic acid, formate production has been neglected. In a similar fashion, the FE towards formic acid has not been taken into account in calculation of the FE towards liquid products as it is not desired. The energy efficiency is computed regarding liquid products only, formic acid has been taken into account within this metric as it is part of the product mix.
Based on the values from Table 2.2, a minimum faradaic efficiency towards liquids of 40% is taken as the minimum desired value.

2.4. Cell configurations and components

In this section a more in depth look will be taken into the design of the flow cell and its options. This section will start off by identifying the different cell configurations after which each component of the cell shall be described along with its design options.

A flow cell in CO_2R is observed to have only five architectures to choose from as are depicted in Figure 2.2.

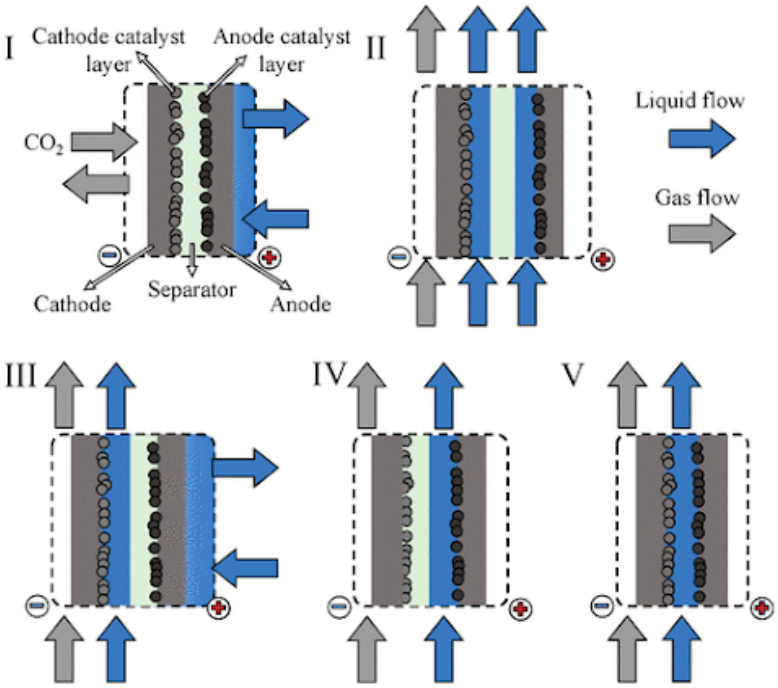

Figure 2.2: Schematic of possible flow cell configurations [58].

As could be observed from Figure 2.2 the different configurations are mostly determined by the presence of electrolyte between an electrode and the membrane respectively. An important abbreviation to know is the Membrane Electrode Assembly, referring to configuration 1 in which no catholyte is present and both electrodes are directly pressed on the membrane. Note that configuration 5 represents a microfluidic cell, this configuration has already been excluded from analysis. Within the following section, each component; the electrode, the catalyst layer, the electrolyte and the membrane will be described along with its design options and its influence on CO_2R.

2.4.1. Electrode

A commonly used archetype of electrode in CO_2R is the gas diffusion layer or GDL and is most commonly carbon-based, a typical build up of a GDE is schematically depicted in Figure 2.3. The main functions of a GDE are to provide a pathway for both gaseous compounds and electrons towards the reaction site, at the reaction site a three phase boundary is created including gaseous CO_2, liquid electrolyte and solid catalyst.
The most simple GDE's are build up out of a Gas Diffusion Layer (GDL) and a catalyst layer. The GDL functions to control water, reactant and electron flux towards the catalyst layer. The catalyst layer functions to facilitate the three phase boundary to enable reduction and shall be further elaborated upon in subsection 2.4.3. The most important parameters of GDL's are the following [38],[34]:

- Gas permeability, related mainly to the overall pore sizes and thickness of macro-porous layer.
- Hydrophobicity, related mainly to PTFE content in the micro-porous layer
- Conductivity, related to the PTFE content.

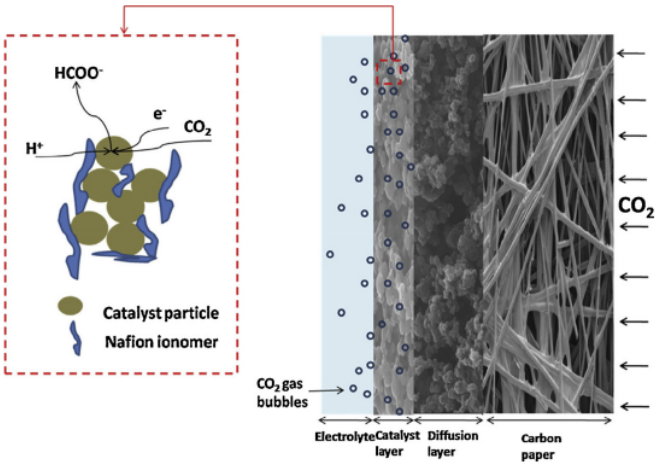

Figure 2.3: Schematic of a gas diffusion electrode [38].

2.4.1.1 Failure modes

In order to design a proper stable GDE it is important to understand its failure modes. The most prominent failure mode is flooding, defined as electrolyte protruding through the pores of the GDL reducing mass transfer of CO_2 and thus CO_2R activity [14]
In general the adversion to flooding of a GDE is managed by the hydrophobicity of said GDE and almost all causes of flooding can ultimately be reduced to a decrease in hydrophobicity. Common ways to increase hydrophobicity of a GDE are to increase the ionomer content of the catalyst layer, increase the PTFE content within the micro-porous layer or increase the pore size [34].

Multiple cumulative flooding mechanisms may be occurring simultaneously [73], it is therefore necessary to understand the different processes and identify its solutions.

A first prominent phenomenon within flooding is the formation of carbonate salts such as $KHCO_3$ and K_2CO_3. These salts form due to the reaction of CO_2 with CO_2R generated hydroxide ions resulting in carbonate, presence of cations such as K^+ enables the formation and precipitation of these (bi-) carbonate salts. The hygroscopic (bi-) carbonate salts cause flooding upon precipitation by drawing electrolyte into the GDE [35] [61]. Dependencies include the electrolyte pH and the concentration of cations such as K^+. Solutions include periodic flushing with deionized water [59],[8], and temporary reduction of current density [72]. Both of these solutions were only proven for MEA's and microfluidic cells.

It was reported that carbon paper gradually becomes more hydrophilic over time due to an increased presence of oxygen atoms in the form of OH and COOH groups at the carbon surface [7]. To omit this problem the authors of the cited report utilized a PTFE membrane instead of carbon paper.

Another theory on the flooding phenomenon is reported by [73] who hypothesise that HER activity on exposed carbon particles locally reduces the capillary pressure leading to the flooding of the GDL. As such the theory hypothesis that the on-set potential of HER on carbon paper is a key measurement, the lower on-set potential associated with the acidic environment might thus be the cause. A possible solution would be to reduce the amount of exposed carbon particles. Another potentially related flooding mechanism is due to electrowetting of the carbon paper.

One last effect worth mentioning is the decrease of surface tension of an electrolyte with rising concentration of alcohols again promoting flooding [73] [76], the most obvious solution to this problem is by keeping the concentration of ethanol low.

2.4.1.2 Types

Typically two types of GDL are used, carbon paper based GDL's as schematically depicted in Figure 2.3 and PTFE membrane.
Advantages of GDE's based on carbon paper include high conductivity, therefore homogeneous cur-

rent distribution, and the relative stability of catalyst layers. Disadvantages include the high costs of the material and relatively low mechanical and chemical robustness [14]. Another disadvantage is that the hydrophobicity of carbon GDE's might not be sufficient requiring additional layers to prevent flooding as mentioned above.

Another often used material is PTFE,commercially known as Teflon, a very thin porous membrane between 20 and 300+ µm thick [26]. As PTFE is non-conductive, electrons are provided by a path directly to the catalytic side of the GDE. No distinction is made between a macro or microporous layer. The most important adjustables parameter of PTFE membranes are pore size and thickness, a thinner membrane was related to larger CO_2R activity and a lower applied voltage [26], commonly found pore sizes are 220 and 450 nm.
[61]. This material is known for its strong hydrophobicity and chemical robustness, thereby reducing the chance on flooding. Another effect worth mentioning on hydrophobicity is that it might induce increased formation of C2+ products by reducing the amount of catholyte present within the catalyst layer, this effectively creates a larger reaction surface vs electrolyte ratio and thereby reduces the pH [3] [71]. On top of that, the material is cheap compared to carbon paper enabling potential industrial production and scaling [14]. The main disadvantage of PTFE membranes is its poor conductivity [35] requiring electron provision from the front of the GDE. Solutions to the poor conductivity include addition of an additional conductive layer [14]. Physical scaling of PTFE membrane based systems is still an immature research topic however solutions are available [11], [27]. It should be noted that the distribution of current density over the catalyst layer in a PTFE based membrane might not be perfectly homogeneous as the conducting layer might not be perfectly homogeneous. This reduces the utilization rate of catalysts. This problem could be solved by interposing additional carbon nanoparticles between a Cu-based catalyst layer and a graphite layer acting as current collector [7]. A conductive top layer is not required, some reports utilize the conductivity of the catalyst layer itself, often in the case of a sputtered copper layer [76].

2.4.1.3 Overview

To summarize, although carbon based GDE's are widely spread within research on electrochemical cells these GDE's may inherently induce stability problems at high cathodic potentials as expected in acidic cells. On the other hand, an exchange with a PTFE based membrane might solve the flooding problem but often requires additional layers of carbon to compensate for its low conductivity, the efficiency of the cell is generally reduced compared to carbon based GDE's. The advantages and disadvantages of both materials have been summarized in Table 2.3. Although PTFE yields many advantages, its immaturity regarding physical scaling of the GDE led to the choice of carbon-based GDL's.

	Carbon paper	**PTFE**
Adversion to flooding	Lim. Hydrophobicity at increased potentials	High
Chemical stability	Medium	High
Mechanical stability	Medium	High
Conductivity	Conductive	Requires additional layer
Current distribution	Homogeneous	Requires layer modifications
Cost	Medium	Low
Maturity	Medium	Low

Table 2.3: GDE material properties [14],[73]

2.4.2. Electrolyte

Electrolyte in electrochemical cells is defined to be a component supporting transfer of ions, and therefore being charge conductive while being electrically insulating [2]. The electrolyte and its ion transport completes the electrical circuit and is found to have a significant influence on the performance of the cell. Disregarding the electrolytes for other types of cells such as molten salt electrolytes and the electrolyte used in SOEC's, two main types of electrolytes can be distinguished within flow cells: aqueous and non-aqueous electrolytes. Two advantages of non-aqueous electrolytes such as acetonetryl and methanol include a high solubility of CO_2 and a reduced amount of protons decreasing the competing

hydrogen evolution reaction (HER) rate [1]. The first advantage however is omitted via the use of a GDE while the second is proven to be unwarranted as low HER has been achieved in aqueous electrolytes as well. Due to the low conductivity and low technology readiness level (TRL) of non-aqueous electrolytes the remainder of this report will focus on aqueous electrolytes.

2.4.2.1 Influences of electrolyte characteristics

Three characteristics of the electrolyte with a notable influence on the yield of an CO_2R reaction cell are the following.

1. pH
2. Cations & anions
3. Conductivity

2.4.2.2 pH

The pH of the electrolyte has a large influence on the performance of an electrochemical cell. It has been widely established that a more alkaline environment results in a higher faradaic efficiency towards C2+ products. As the cathodic environment becomes more acidic, more protons are available. These protons can reduce at the cathode to form hydrogen via HER, an acidic environment has been associated with methane formation as well. These parasitic reactions occurs alongside the carbon reduction reaction and thus decrease the FE towards desired liquid products.
The influence of pH on ethanol/ethylene yield ratio is demonstrated by [75] as depicted in Figure 2.4a. Furthermore it was shown that the on-set potential of CO and C_2H_4 was significantly reduced in a more alkaline environment as is depicted in Figure 2.4b [7].

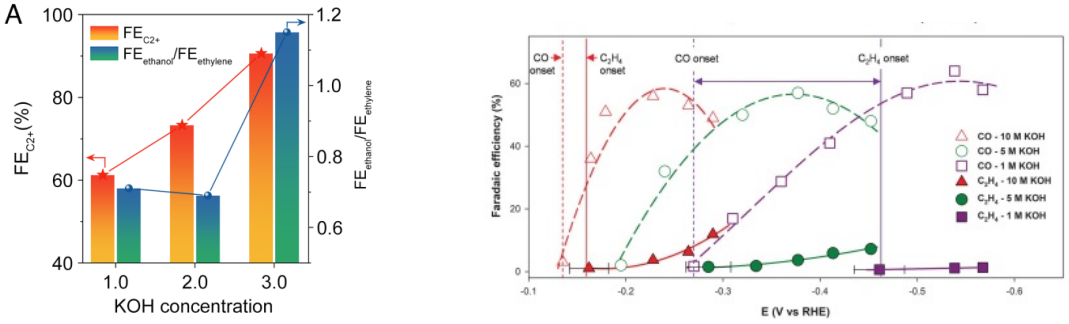

Figure 2.4: a) Influence of pH on the ratio between ethanol and ethylene. **b)** CO_2R on-set potential dependence on alkalinity [7].

Having established the importance of alkaline conditions to decrease HER and methane formation, two other aspects are vital to consider.
Firstly the local pH at the surface of the cathode, as CO_2R produces OH^- ions, a large current density could generate and maintain a highly alkaline layer at the cathodic surface. [57] cites a pH difference over 6 points between the cathodic surface and a neutral bulk pH whereas a model proposed in [23] shows an alkaline local pH up to a value of 12 at current densities above 400 mA within an acidic electrolyte with a pH of 1. Experimental determination of local pH has shown to be hard although [57] proposes the use of very strong buffers, the application of this method has not been observed in literature. This local pH is highly dependent on the electrolyte composition and already in 1989 [22] noted a difference in selectivity caused by anion selection. It was discovered that non-buffering anions enhanced selectivity towards C2+ products compared to buffering anions in the following order Cl^->ClO_4^->SO_4^{2-}>HCO_3^->HPO_4^{2-} [30],[45]. Upon further investigation two theories were defined, the first relates the buffering capabilities of the anion to the local pH formed at increased current densities. The buffering capacity reduces the local alkalinity, thereby enabling more HER and methane formation [22]. A second theory states that a second mechanism is at play on top of the first mentioned, it states the buffering anions considered can function as a proton donor for HER and methane formation directly on the surface of the cathode [52]. Regardless of the mechanism(s), the conclusion is the same and

buffering electrolytes should be avoided to reduce HER and increase C2+ product selectivity. The influence of a buffering electrolyte is depicted for bicarbonate in Figure 2.5. As could be read from the graphs, methane and hydrogen formation is increased with increasing buffer capacity [57].

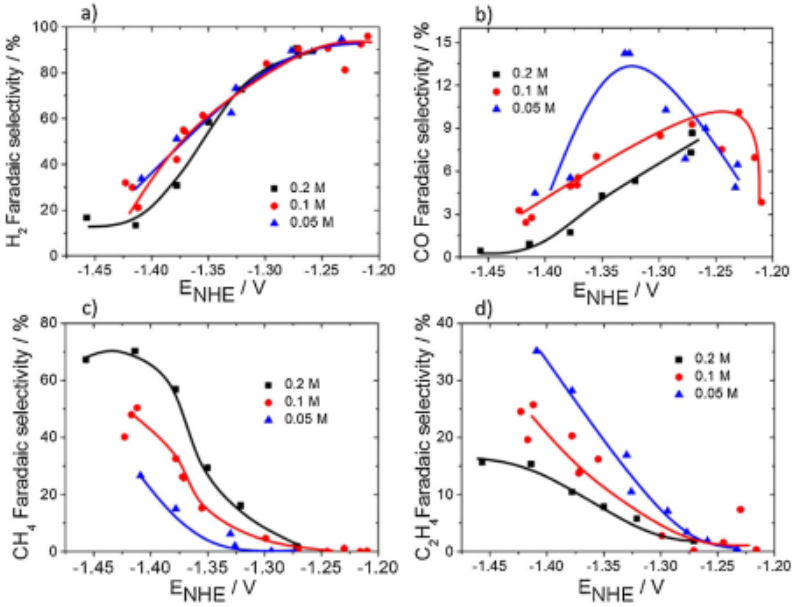

Figure 2.5: Graphically depicted the influence of a buffering electrolyte, in this case $KHCO_3$ [57].

Other manners to increase the local pH at the cathodic surface such as the addition of a layer on top of the catalyst layer or utilizing a porous catalyst structure are described in more detail in subsection 2.4.3.

The second aspect to consider is the solubility of CO_2 in neutral and alkaline electrolytes. Above a pH of 4 CO_2 will form carbonates upon dissolution, destabilizing the electrolyte [1] [13].

To indicate to what extend CO_2 dissolution is a problem in alkaline solutions, the absorption rate of CO_2 in an 7 M KOH solution is around 10 times faster then a 100% selective conversion rate towards ethylene at 250 mA/cm^2 [50]. Due to this process the performance of neutral and alkaline electrolytes degrades over time thereby requiring a regeneration process. It should be noted that carbonate salt precipitation as described in subsection 2.4.1 is caused by this same mechanism. Additionally the dissolution of CO_2 within the electrolyte will severly affect the CO_2 utilization rate.

A last aspect to consider is the restraints imposed on the membrane by the electrolyte pH. A highly alkaline electrolyte significantly reduces conductivity of a cation exchange membrane as the concentration of protons is low,the opposite mechanisms explain why anion exchange membranes are not used in acidic environments. The choice of electrolyte is thus not solely based performance of CO_2R but all effects on cell level should be taken into account, the consequences of electrolyte choice on cell level shall be further elaborated upon in section 2.5.

2.4.2.3 Cation & anions

From literature it is observed that the choice of cation has a significant effect on the performance of the cell. It is reported and proved that larger cations, ranging from lithium, sodium, potassium to Caesium, result in an increase in both the CO_2R activity in general and C2+ products yield [22][30]. It is believed that this trend is explained by a decreasing hydration number with increasing size, in other words; a smaller amount of water molecules are bound to Cs^+ compared to Li^+. This leads to easier adsorption on the catalyst surface, creating a more positive potential in the outer helmholtz layer, effectively repelling protons [22]. Additional theories suggest that the electrostatic field associated with the cations increase both $*CO_2$ stability and promote C-C coupling, a vital step in the production of C2+ products [45].To illustrate the importance and significance of cation choice within the electrolyte,

Figure 2.6a below shows the partial current densities of compounds within CO_2R in alkali bicarbonates at a constant voltage, especially ethanol and ethylene are seen to increase with increasing cation size.

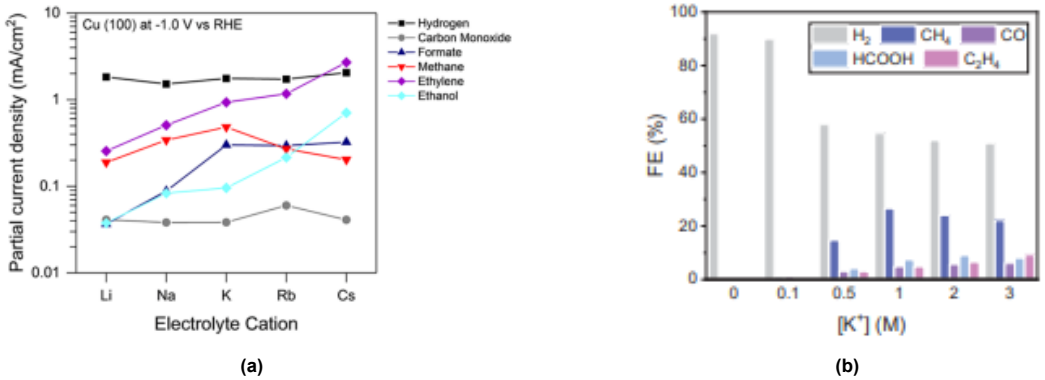

Figure 2.6: a) Illustration of the importance of the cation choice, the electrolyte consisted of 0.1 M XHCO3 [1]. **b) The influence of cation presence within the electrolyte, in this case within an acidic environment [23].**

To further demonstrate the need for alkali metals within the electrolyte, Figure 2.6b shows how selectivity is altered by addition of alkali metals containing neutral salts without altering the pH or buffer-capacity of the electrolyte. Other reports report a more significant change. For example, an increase in FE to C2+ products from 0% towards 80% by addition of up to 3 M KCl to the electrolyte was reported in an acidic cell [24]. It should be noted that addition of neutral salts such as KCl also increases the conductivity significantly leading to reduced voltages. The cell considered in the figure is an acidic cell, however the effects are believed to extend towards neutral and alkaline environments. It should be noted that addition of alkali metal salts to the electrolyte until 3 M K^+ is not observed to be common among neutral and alkaline based electrochemical cells, this might be due to carbonate formation causing flooding.

Considering the anions, as was mentioned within the paragraph about pH, buffering anions should be avoided to enable a high local pH. Secondly within the group of halides a trend has been observed regarding its influence on CO_2R. An increased negativity of the halide (F, Cl, Br, I) within the electrolyte salt provided an increased current density with constant faradaic efficiencies[41].

2.4.2.4 Conductivity

One of the main functions of the electrolyte is to conduct ionic current to close the electrochemical circuit, conductivity is thus an important feature of an electrolyte. The conductivity of an electrolyte is dependent on the amount of free ions and therefore imposes additional design constraints. This is exemplified by an electrolyte consisting of $KHCO_3$, on one hand a lower concentration will reduce the buffering effect improving C2+ yield, on the other hand it will increase the resistance of the cell due to conductivity issues. Similarly in acidic cells, a higher concentration acid will be more conductive but will also increase HER and methane formation. Within the catholyte of acidic cells, as described before, neutral salts such as KCl are often added to improve conductivity. Important to notice is that addition of halide based salts in the anolyte will lead to the production of unwanted gasses upon oxidation. As a pH gradient over the membrane is unwanted the pH of both the catholyte and the anolyte is thus connected to the conductivity of the anolyte.

2.4.2.5 Overview

Summarizing the foregoing paragraph, the pH has a large influence on the performance of the cell and CO_2R towards ethanol is most favourable in an alkaline environment. This could be provided either by use of an alkaline bulk electrolyte or by creation of a high local pH. Alkaline and neutral electrolytes degrade over time by dissolution of CO_2 while simultaneously enabling carbonate salt precipitation. Considering the specific ions in the electrolyte, alkali metals are the cations of choice promoting C2+ product formation with Cs as the optimal choice. The anions must not posses any buffering capacity, one possibility would be to use halides of which Iodide is expected to be most beneficial to the

performance of CO_2R. In light of the research question which focuses on stability and reduction of downstream processes, alkaline and neutral electrolytes seem a less good fit.

2.4.3. Catalyst layer

The faradaic efficiency of an electrochemical cell is heavily influenced by the structure and composition of the catalystlayer. Within this section a short introduction shall be given on the different catalysts commonly used in CO_2R towards alcohols and C2+ products.

2.4.3.1 Materials

Metal based-catalysts is the largest and most commonly used group of catalyst. Noble metals such as Au, Ag and Zn have been found to produce mainly CO, metals including Pb, Sn and Bi selectively produce formate whereas until now only copper was observed to produce C2+ product in larger quantities [1]. Still, within the domain of copper based catalysts there is a large variety of selectivity possible enabled by, among other factors, changes in nanostructure, electronic structure and addition of impurities [1], [30],[64]. Another important category is the class of oxide derived catalysts.
Arguably the most interesting variation on the catalyst layer is by addition of impurities which can significantly increase both the selectivity towards C2+ products as the ratio of ethanol over ethylene. One prominent theory describes the use of for example silver, thereby increasing *CO coverage and enabling a process called spillover Within this process the adsorbed *CO ”hops” from a silver lattice towards a copper lattice before further reducing towards ethanol [30]. Alternatives to the spillover theory describe how selectivity towards ethanol is increased by stabilization of oxygen containing intermediates and *CO [20] [70], some report that is due to an increasingly oxophilic catalyts layer [6]. Regardless of the exact mechanism, the effect is depicted in Figure 2.7a, it is clearly shown how the silver content within the electrode enables a selectivity increase from just above 20% towards 40%. The researchers who designed the cell attributed this high selectivity to the stability of $*OC_2H_5$ caused by the variety of binding sites for *CO [63]. A similar effect is associated with pyridinic nitrogen doped carbon, [20] showed a faradaic efficiency towards alcohols of 73%, although at current densities around 10 mA/cm^2, attributing the high selectivity on the spillover mechanism described above. Table A.2 shows two cells with a high amount of pyridinic nitrogen, both yielding a high faradaic efficiency towards ethanol of 45 [6] and 52% [66]. Both associated the high selectivity towards ethanol on a higher binding strength of CO and oxygen containing intermediates, preventing deoxygenation.

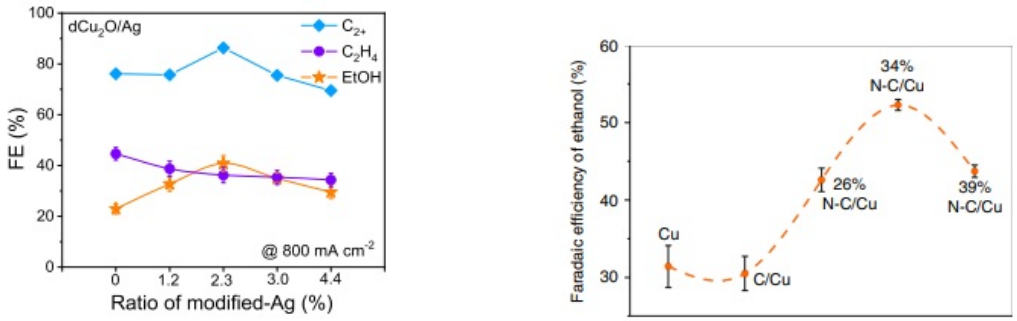

Figure 2.7: a) Effect of addition of Ag on selectivity within a neutral cell [63]. **b)** Effect of addition of pyridinic nitrogen to the catalyst layer on ethanol selectivity [66].

An important note is that the quantities in which these materials are added all show an optimum, optimization is therefore a requirement.

A last type of impurities within the catalytic layer are hydrophobic materials, these can reduce the concentration of catholyte within the catalyst layer and thereby increase the availability of CO_2. [71] attributed an enhanced CO_2R current density to an increased mass transport of CO_2 due to a pore like structure created by adding PTFE to the catalyst ink. Additionally the same phenomenon was proven in acidic environment in [74]. The effect of hydrophobicity of the catalytic layer is supported by [74] which

states that hydrophobicity is a key factor in suppressing HER in acidic cells and showed via simulations that it had a positive effect on the migration of OH^- ions. Thereby effectively increasing the local pH on the cathode surface and thus by extension the selectivity towards ethanol. The relation between hydrophobicity and C2+ product generation was depicted via the graph shown in Figure 2.8. This was experimentally supported in K_2SO_4 catholyte by creating a custom made carbon based GDE with high content of PTFE, additionally PTFE was spray-coated along with the catalyst during fabrication of GDE. An important note provided in the report is that the hydrophobicity of bare carbon based copper GDE's significantly decreases during operation; thus to examine the influence of hydrophobicity with accuracy it is necessary to evaluate the contact angle both before and after operation.

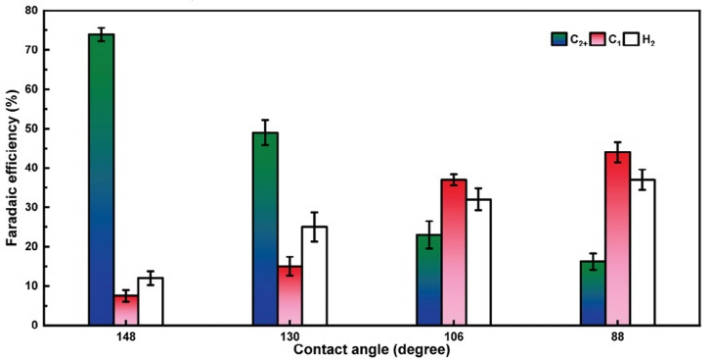

Figure 2.8: Effect of hydrophobicity of catalyst layer on C2+ product generation, test performed in K_2SO_4 (pH=2.0) [74].

The addition of hydrophobic impurities was also shown to affect the ratio of ethanol over ethylene, a Polyvinylidene fluoride (PVDF) binder was utilized to increase the hydrophobocity minimizing the amount of protons on active catalytic sites. A severe increase in ethanol/ethylene ratio was found [4].

2.4.3.2 Additional layer

An additional layer on top of the catalyst layer could increase faradaic efficiencies towards CO_2R, four distinct roles have been observed throughout literature; to increase the local pH, to increase the presence of alkali metals, to catalytically improve CO_2R and lastly to provide a conductive path for electrons. It should be noted that although not exclusively, additional layers have been observed primarily within acidic and neutral cells.

Increment of local pH

First of all the increment of local pH, numerous reports have been published in which a hydrophobic layer consisting of, among others, materials such as PTFE, graphite-oxide and 1-octadecanethiol were applied with the effect of decreasing HER [14]. The effect was demonstrated in a neutral $KHCO_3$ environment [37]. The article cited experimented with multiple different hydrophobic materials such as PVDF and perfluoroalkoxy alkane (PFA) and found a significant increase of C2+ products, attributing this effect to restricted water diffusion, ultimately increasing the pH as CO_2R inherently creates an alkaline environment.

It is unclear to what extent hydrophobicity could increase the ethanol over C2+ product ratio, extending the relation between local pH and hydrophobicity it is suggested that the ethanol over C2+ ratio could be increased by addition of hydrophobic layers.

Alkali presence

To increase the presence of alkali metal ions The mechanism utilized was based on the higher affinity of K+ towards sulfonate groups (-SO_3^-) compared to protons, while protons are reacted away by the catalytic reaction, potassium ions are stabilized. Specifically Aquivion PFSA was used with a molecular weight of 790 g/mol to increase the sulfonate group content within the layer compared to the more heavy Nafion variant (1100 g/mol). Secondly the orientation of the molecule was hypothesised to allow for gas transport via the hydrophobic $-CF_2$ groups to prevent blistering of the layer. While testing the influence of the PFSA content on the faradaic efficiency, the authors also showed that this mechanism was independent from the hydrophobicity based mechanism, suggesting both work simultaneously. An

important note on the top layer described above is the importance of correct molecular configuration, the molecular configuration was managed by addition of another ionomer in the PFSA layer, a wide variety in performance was found between the ionomers tested, the performance described was managed by addition of a covalent organic framework. A second example of a negatively charged top layer with the aim of stabilizing alkali ions is the utilization of a charged $EMIMBF_4$ layer [60]. The layer is shown to increase the yield of C2+ products severely at all current densities, however no comparison is made with a neutral hydrophobic layer. It is to be noted that both of the above mentioned articles utilize an acidic electrolyte.

Catalytic effect
As was mentioned before, some additional layers are applied with a catalytic effect. The addition of a doped carbon layer with pyridinic nitrogen was reported to severely increase faradaic efficiency towards ethanol from around 30% on pure Cu to above 50% [66].

Stabilization and conductivity
Lastly a carbon black or graphite layer is often added on top of the catalyst layer if a PTFE GDE is used to compensate for the poor conductivity of PTFE and stabilize copper catalysts on the membrane [7].

Downsides
A few downsides are associated with the addition of an extra layer on top of the catalyst layer, first of all a minor increase in resistivity is observed. Secondly, in the case of carbon based layer, it was reported that the hydrophobic effect was reduced below -0.6V vs RHE and the layer lost its working mechanism [26]. Again this phenomenon must be treated with caution as other reports did not observe this [23]. Another degrading mechanism observed after addition of a carbon layer is the detachment and reattachment of Cu particles from a PTFE membrane towards the carbon layer, this phenomenon was hypothesised to result in increased HER activity [76]. Lastly it was reported that a carbon layer on top of a Cu layer could increase the energy barrier for *CO dimerization [66], a crucial step in C2+ product formation. Note that most of these downsides are related to the use of carbon based compounds.

2.4.3.3 Overview
In conclusion, the catalyst layer has an incredible effect on the selectivity of the cell and many parameters could be altered to increase selectivity towards ethanol. Two manners regarding the material stand out. Firstly increasing impurities within the catalyst layer, especially with CO producing compounds such as Ag, Pd, Zn and pyridinic nitrogen can significantly enhance the selectivity towards ethanol and should be evaluated carefully to find the optimum quantity.
An additional layer can significantly change the selectivity as well, this could be an additionally coating of ionomer or a carbon layer. One of the main mechanisms of this additional layer is the regulation of ion migration, both by active groups and by increasing hydrophobicity. Secondly an additional layer can contain catalytic compounds to further increase the faradaic efficiency towards ethanol. An additional (partly) carbon layer could additionally be used to provide a homogeneous current distribution on PTFE membrane based GDE's [23].

2.5. Cell design
Within this section, the information described in section 2.4 will be combined to formulate a number of cell designs for the direct conversion of CO_2 towards ethanol. In order to structure the cell design process, this section has been subdivided into 3 paragraphs, an AEM based cell optimization, a cation exchange membrane (CEM) based cell optimization and a concluding paragraph in which the cells and the expected potentials are compared. The cell configurations to be considered are depicted in Figure 2.2, all cells considered are classified in the following manner: #of configuration, Membrane (C for Cation and A for Anion exchange membrane), pH of catholyte (high for alkaline, N for neutral, L for acidic) and similarly the last letter stands for the pH of the anolyte.
Note that configuration 5 has been excluded from further analysis as it is a microfluidic cell. Additionally based on low TRL, stability of bipolar membrane based cells and low energy efficiency [1], bipolar membranes have been excluded from this cell design. It should be noted that both in forward bias [43] and reverse bias [60] interesting results have been achieved concerning ethanol extraction concentration

and CO_2 utilization.

Some additional remarks must be made with respect to the cell design; first of all, with an eye on the downstream process a low concentration of ethanol might significantly alter the energy required for extraction. As is described in Table 2.4, an incredible amount of energy is required to distillate ethanol at low concentrations increasing rapidly with reducing concentration. Note that the HHV of ethanol is 29.7 MJ/kg.

	Distillate [w%]/ Source		
	90/[15]	93/[44]	95[25]
Feed [wt%]	**Energy [MJ/kg]**		
1	45	26	36
2	22	15	20
10	4.7	7	5

Table 2.4: Ethanol distillation energy requirements

Secondly, the regeneration of electrolyte after dissolution of CO_2 is commonly done by thermal calcination, a very energy intensive process [14].

2.5.1. AEM based cells

Anion exchange membrane based cells support the migration of anions or negative ions. This type of membrane as opposed to CEM's are directly fit to provide an alkaline environment for the OER and are often used in combination with an alkaline or neutral anolyte.
Three large themes are considered for anion exchange membranes:

1. CO_2 utilization
2. Ethanol cross-over
3. Electrolyte stability

A large disadvantage however, is the conductance of anions such as HCO_3^- and CO_3^{2-} besides OH^- ions [38]. On the cathode side, CO_2 reacts towards HCO_3^- and CO_3^{2-} and subsequently migrates through the membrane towards the anode where it oxidizes to CO_2. Migration of other neutral compounds such as ethanol are reported to be partly induced by this same ion flux towards the anode. The phenomenon of migration of carbon containing molecules is called CO_2 pumping and is one of the main drawbacks of AEM's as it leads to a low conversion rate of CO_2 and reduced efficiencies.

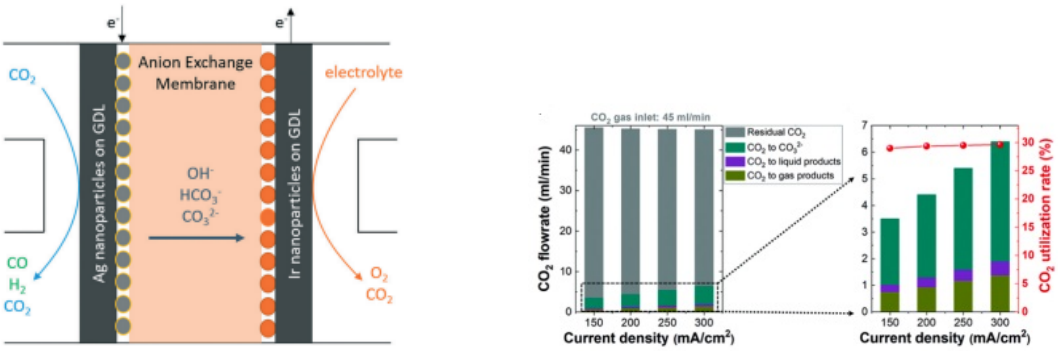

Figure 2.9: a) CO_2 pumping through carbonate migration [31]. **b)** Exemplified CO_2 utilization rate in MEA aimed on CO [1].

Reports have shown that (bi-) carbonate is the main transport species in both MEA configurations [31],[9] and flow cell configurations with a catholyte [10]. In the case of carbonate being the only transport species, a maximum CO_2 utilization rate of 50% can be reached as for each pair of electrons one carbonate ion must migrate. Similarly for ethanol only a maximum utilization rate of 25% is possible

with CO_3^{2-} as only transferspecies [42].

Considering the crossover of ethanol, although little is known about cells following configurations 2 and 3, multiple sources show its severity in MEA's.
Simulations showed that in MEA based cells the ratio of cathodic over anodic output of ethanol would be between 0.45 and 1.5 depending on temperature and current density indicating large crossover of ethanol, both the temperature and current density increased the cathodic yield with increasing values [42]. Additionally MEA configuration as are reported to cause severe ethanol crossover of 75% to 80% [43], [13],[35]. A test set-up with an AEM based MEA aimed to produce hydrogen, at an anolyte concentration of just 0.5 wt% ethanol and a current density of 200 mA/cm^2 yielded that ethanol oxidation provided 20% of the electrons, highlighting the severity of ethanol crossover [43].
Based on the severe ethanol loss associated with these type of cells, configurations 1 and 4 are excluded from further examination.

Considering configurations with a catholyte such as 2 and 3, severe electrolyte degradation was shown to be present for all mentioned electrolytes [13], [40]:

1. KOH
2. $KHCO_3$
3. K_2SO_4
4. KCl

KOH showed severe conductivity reductions due to formation of carbonates in the catholyte in both configurations 2 and 3. $KHCO_3$ was unstable due to salt precipitation as well. Both K_2SO_4 and KCl showed large pH increments over time, due to migration of the anions, leading to reduced ionic conductivities [13], [40].

To conclude, advantages of the AEM based cell is the possible use of alkaline electrolyte, enabling both cheap anodic catalysts and improved CO_2R performance. A large disadvantage is the inherent degradation of electrolyte due to CO_2 solubility, the CO_2 pumping effect and the increased chance on flooding due to carbonate formation. All of these phenomena induce the need for additional downstream processes.

1. The electrolyte needs to be regenerated to reduce carbonate presence to prevent salt formation
2. CO_2 must be recovered from the gaseous cathode flow from a mixture of H_2, CO and C_2H_4
3. CO_2 must be recovered from the anolyte side in a mixture with oxygen
4. Ethanol concentration within flowcells can not reach high concentrations due to migration

From an overview of current technology, the following characteristics have been deduced. As these characteristics are taken from a small sample, biases can not be excluded. Note that the energy efficiency has not been taken into account, this is due to the fact that all cells described below have reported the cathodic voltage only. All cells in the sample utilize KOH as a catholyte.

Config.	FE H_2	J_liq	FE_liq	FE C2+	Alc./C_2H_4	CO_2->Liq. [%]	Stab. [h]	Source
2AHH	10	175	62	81	2.1	2.7	100	[6]
2AHH	13	46	23	47	0.6	1.7	2	[40]
2AHH	10	352	44	78	1.1	-	6	[63]
2AHH	20	100	50	67	2.6	-	10	[51]
2AHH	13	216	54	59	1.5	-	2,5	[77]
3AHH	8	538	54	91	1.1	1.6	7	[75]
Charac.	**5-20**	**100-500+**	**40-60**	**50-90**	**1-2.5**	**<5**	**5-100**	**N.A.**

Table 2.5: AEM based cell characteristics via the configuration coding as described in section 2.5.

2.5.2. CEM based cells

Cation exchange membranes are conductive to positive ions and are the most mature type of membranes used in electrochemistry due to the utilization within water hydrolysis. It requires an acidic or neutral medium and excludes the absence of a catholyte layer due to proton migration. This is supported by models of the pH gradient in [23] and [70] in which a diffusion layer in the order of magnitude

of 10-100 μm is required to provide an alkaline environment at the catalytic layer at current densities above 500 mA/cm^2, as depicted in Figure 2.10. The reason for discrepancy between both sources on possible local pH at catalytic layers is unknown.

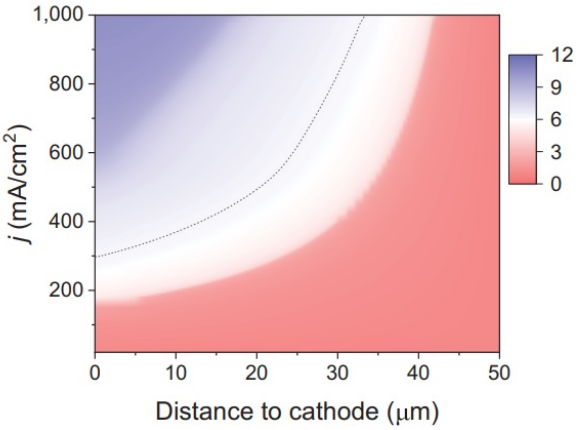

Figure 2.10: pH gradient as a function of current density throughout the catholyte layer [23].

A top layer enables even lower current densities due to the effect described in subsection 2.4.3 and minimal HER was demonstrated at current densities around 300 mA/cm^2 [76] and [60]. Although no literature has been found describing neutral CEM-based cells, it is expected that the anolyte suffers from degradation due to migration of the cation.
Lastly an acidic anolyte requires more expensive catalysts on the OER side.

In conclusion, CEM based cells require a catholyte which would optimally lead to configuration 3 in section 2.4. The acidic cell avoids the solubility problem as could be read in subsection 2.4.2 while the cathodic local pH is suggested to reach strongly alkaline values at elevated current densities. To increase the conductivity within the catholyte and increase CO_2R, additional KCl could be added, this could later be replaced by Cs^+ and I^- to further optimize the electrolyte. Advantages include a high CO_2 utilization up to 77% [23], a stable electrolyte enabling long term operation [23] and a high TRL membrane. The stable electrolyte is believed to be a key feature needed to yield high concentration ethanol. Additionally no reports have been found to date describing ethanol migration through a Nafion membrane. Disadvantages include the low efficiencies associated with the increased current density required, the low TRL of the overall system, the additional voltage associated with maintaining the pH gradient in the catholyte layer of 0.77V [49] and the high catalyst costs compared to the AEM based flow cell.

The downstream processes associated with these cells are summarized below.

1. Ethanol distillation, at a higher concentration compared to AEM based cells.
2. CO_2 must be recovered from the gaseous cathode flow from a mixture of H_2, CO and C_2H_4

Again it was attempted to characterize the cell by means of analysis of cells described in literature in Table 2.6.

Config.	FE H_2	J_liq	FEliq	FE C2+	Alc./C_2H_4	CO_2->Liq. [%]	Stab. [h]	Source
2CLL	42	264	22	40	0.6	6.4	12	[23]
3CLL	5	273	39	79	0.7	-	30	[24]
2CLL	10	76	38	75	0.6	2.4	30	[76]
3CLL	17	-	-	62	-	-	50	[74]
Charac.	**5-20**	**50-300**	**20-40**	**40-80**	**0.5-0.8**	**2-7**	**10-50**	**N.A.**

Table 2.6: CEM based acidic cell characteristics via the configuration coding explained in section 2.5.

2.5.3. Trade-off

Upon comparison of the characteristics of the two types of cells, three things stand out, the CO_2 utilization rate, liquid products produced, which is highly related to the ratio of alcohol over ethylene. Lastly the seemingly large advantages regarding the down flow process streams, especially regarding the extraction of ethanol.

The first point of attention is the CO_2 conversion, the parameter described in the tables is the conversion of CO_2 towards liquid products. For AEM's, as discussed, this is a known problem, the acidic cells reported have a far higher overall conversion but are primarily limited by their low liquid output. Reports have shown to yield similar values at a far lower flow rate reaching above 75% single pass conversion [23], [76].

The second point of attention is the amount of liquid products produced, the overall number is lower in acidic cells and this is again shown in the alcohol over ethylene ratio described in Table A.2 as C2+ product yield are approximately equal. The production of ethanol might thus be problematic in acidic cells. A difference between the cells cited is that the acidic cells all aimed for C2 products whereas the AEM based cells primarily aimed for alcohols specifically. This difference is also observed in the choice of catalyst, cells in the AEM based category all use either doped copper materials [6] [63] [51] or highly porous [40] [75] catalytic materials; acidic cells, with the exception of [70], utilized regular copper.

Regarding the extraction of ethanol, AEM-based cells have a two-fold problem. Firstly, the electrolyte is shown to be unstable in catholyte containing cell type, as the electrolyte can not be looped indefinitely it is unlikely to reach sufficiently high concentration ethanol for extraction. The types of cells which have shown to be stable, of type 1 and 4 have shown to suffer from great ethanol losses around 70%. CEM-based cells have till this moment not shown this ethanol loss and acidic catholytes have been proven to be stable, enabling for higher ethanol concentrations.

Within Table 2.7, a final trade-off has been performed showing the advantages and disadvantages of each cell.

	AEM	**CEM (Acidic)**
Additional process steps required	1. CO_2/H2/CO/C2H4 sep. 2. KOH regen.(cath. & An.) - CO_2 regen. from K2CO3. 3. Low conc. Liq. sep. 4. Anodic CO_2/O2 sep.	1. CO_2/H2/CO/C2H4 sep. 2. High conc. Liq. sep.
Current densities	High	High
Cell Efficiency to liq.	Medium	Low
Membrane stability	Medium	High
CO_2 conv.	Low	High+
Catalyst costs	Low	High
TRL/"risk"	Medium	High

Table 2.7: Comparison of AEM and CEM (Acidic) membranes.

Due to above listed reasons a monopolor acidic cell was deemed to be the design with the highest potential and will therefore be pursued in the remaining of this report. An impression of the cell and its mass flows is shown in Figure 2.11.

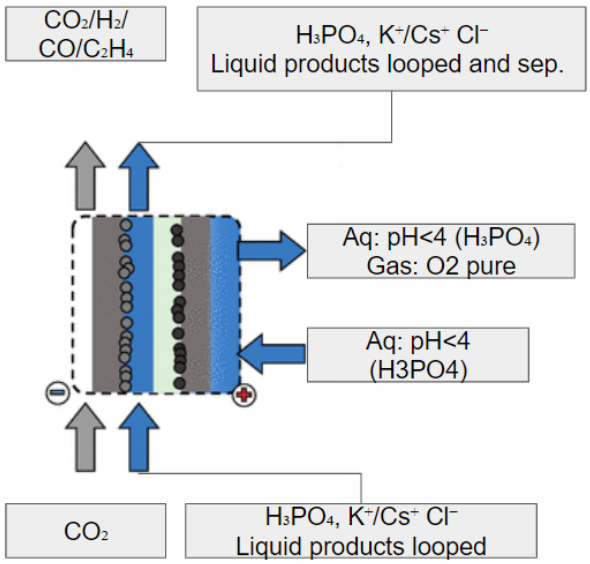

Figure 2.11: Acidic cell and its mass flows graphically depicted

Considering the electrode, a carbon-based GDL was chosen due to the higher maturity on the to be tested cell dimensions. It should be noted that all acidic cells referenced within this report but [74] boasted a PTFE membrane. The exception cited created a substrate similar to a PTFE membrane by adding a PTFE based micro-porous layer. As described in subsection 2.4.1, a large potential is seen for PTFE based membranes as catalyst layer substrate and this could be pursued in a later stage.

Regarding the catalyst layer, as described in subsection 2.4.3, hydrophobocity is a key characteristic for efficient CO_2R. Based on the findings described hydrophobic impurities were the approach of choice to increase performance. This research focuses only on the addition of PTFE within a GDE. Additionally after analysis of described acidic cells it was noticed that, apart from [74] and [70] which operated in a pH of 2, all reports utilized a top layer on top of the catalyst layer. As described in subsection 2.4.3, this top layer could fulfill a number of functions. A noticable silver lining is the hydrophobicity of this top layer reducing proton presence at the catalyst layer. PTFE has been the compound of choice due to its strong hydrophobicity, chemical stability and insulating properties, ensuring no activity within CO_2 reduction.

Considering the electrolyte a clear pattern was observed throughout literature, a strong acid is necessary to maximize the local pH. For comparison with literature, 1 M H_3PO_4 is chosen although H_2SO_4 holds promise as it is a stronger acid. 3 M KCl shall be added to the catholyte.

Looking at options such as an electrolyte of prepared with K_2SO_4 and H_2SO_4 as found in Table A.2. Preliminary experiments with a solution of 0.5 M KH_2PO_4/0.5 M H_3PO_4 and 2.5 M KCl as a catholyte and 0.5 M KH_2PO_4/0.5 M H_3PO_4 as an anolyte resulted in significant salt formation and pH differences due to potassium migration towards the cathode. It was hypothesised that the use of electrolytes as described above would both limit the addition of KCl and reduce stability of the cell. Therefore this report opted for the electrolyte chosen. A more thorough research regarding this subject should be conducted.

3

Research questions and methodology

As indicated in chapter 2 this research opted for an exotic and little researched type of cell, a CEM-based cell with an acidic electrolyte. This introduces the need for the creation of a high local pH. The following manners were identified to increase the local alkalinity:

- Elevated current densities
- Hydrophobic GDE (GDL, catalyst layer and top layer)
- Non-buffering catholyte
- Porous catalyst structure

Within this research, the first two manners shall be evaluated.

As acidic cells are an immature field many questions still reside, involving scalability, performance and stability. Within this chapter a number of knowledge gaps shall be highlighted leading to the research questions as described. The research questions shall be introduced after which the justification further elaborates on its necessity.

3.1. Research questions and justification

3.1.1. Research questions

subsection 2.4.1 introduced the difficulty regarding the up-scaling of PTFE membrane due to its insulating properties. Although progress is made, it is unclear to what extent these solutions might enable large scale PTFE membrane based electrolysis. Therefore, within this report, it will be examined if a sigracet 39BB carbon paper could be utilized for CO_2 reduction in strong acids. This leads to the following main research question:

Could a regular commercially bought carbon based GDE with 0.7 mg/cm^2 Cu and an area of 5 cm^2, be modified for CO_2 reduction towards C2+ products with a Faradaic efficiency above 40% in highly acidic conditions via hydrophobification by addition of PTFE beneath, within or on top of the catalyst layer?

Note that a shift has been made from ethanol towards C2+ products. Due to the limited maturity of acidic cells and the close resemblance in reaction path between C2+ products and ethanol as shown in Figure A.3, this was deemed a logical first step.
The main question is split up in a number of subquestions as listed below. Please note that two different PTFE additives have been utilized within this process, PTFE NP and 60% PTFE dispersion, the specifics are further elaborated upon in section 3.2.

1. How does a PTFE additive based layer on a sigracet 39BB GDL affect the flooding, voltage and FE within a highly acidic (pH=1) environment at a current density of 150 mA/cm^2?
2. How does a PTFE additive based top layer influence the flooding, voltage and FE towards C2+ products in a highly acidic (pH=1) environment at a current density of 150 mA/cm^2?

3. How does addition of PTFE NP within the catalyst layer affect the flooding, voltage and FE towards C2+ products in a highly acidic (pH=1) environment at a current density of 150 mA/cm^2?
4. How does an increased current density affect the FE towards C2+ products in a highly acidic (pH=1) environment?

Additionally, two other research questions have been identified during the research period:

5. Could a spray-coated Cu copper layer be stabilized within a highly acidic (pH=1) electrochemical cell?
6. What are the main causes of performance instability of a Sigracet 39BB based cell with a PTFE based baselayer, Cu/PTFE catalyst layer and a PTFE disp. top layer and how can the stability be improved?

3.1.2. Justification

A major problem during preliminary experiments was shown to be flooding of the GDE, as discussed, flooding decreases the mass flow of CO_2 towards the catalyst and could thus have a significant influence on the performance of the cell. Flooding was shown to be present at current densities as low as 50 mA/cm^2 within an acidic electrolyte. Comparing this data with the failure modes of flooding as described in subsection 2.4.1; formation of carbonate salts, oxidization of carbon paper, HER activity on the carbon particles and electrowetting, only one potentially satisfying cause is identified. The formation of carbonate salts is of course excluded due to the presence of acid, the oxidization of carbon paper could be excluded due to the time span after which the paper starts to flood and electrowetting was excluded as the paper flooded at low current densities. HER activity on the carbon particles would be affected due to the acidic medium and thus could be the reason. Additionally as described in subsection 2.4.1 almost all reported flooding mechanisms depend on a decrease in hydrophobicity, simply increasing the hydrophobicity of the GDL might thus be a solution. This would also prevent flooding due to HER activity as less carbon would be exposed. It should be noted that a similar approach is utilized by [74]. Therefore this research opted to evaluate the influence of application of a PTFE-based layer on the GDL before application of the catalyst layer.

As described in subsection 2.4.3, most acidic cells utilized a top layer on top of the catalyst layer. Apart from other functions such as conductivity and alkali presence as described, this top layer will only act to reduce proton transport towards the catalysts via its hydrophobicity. The evaluation of the influence of adding a highly hydrophibic top layer is thus critical for the development of these acidic cells.

Addition of PTFE NP within the catalyst layer are shown to have a significant effect on the FE towards C2+ products in $KHCO_3$ as described in [71] and in acid as described in [74]. This strongly suggests a similar working within an environment of pH=1.

Another problem found during preliminary experiments was the stability of the copper catalyst layer. No data has been found regarding this subject within literature on acidic cells. As copper stability is a crucial part of the CO_2 reduction, examining this problem, its causes and its solutions is a prime research subject to be evaluated.

3.2. Methodology

Within the remainder of this report a distinction is made between the three main subjects. The first 4 sub-questions are evaluated in a series of tests later to be referred to as ”Flooding tests” and ”CO_2R tests”. The 5th sub-question and its corresponding experiments will be referred to as ”Catalyst stability’. Within each chapter, a short description on the custom set-up used for the specific tests will be described along with an overview of the experiments concerning the specific subject.
The following section will provide a general description of the test set-up and the utilized equipment.

3.2.1. Test Set-up

3.2.1.1 Anode build up

A platenized titanium mesh was spray-coated with an ink consisting of the following materials.

- 60 mg IrO_2 nanoparticles
- 1.5 ml of ultrapure water
- 1.5 ml IsoPropanol
- 150 µl Nafion 1100 5wt% solution.

An additional heat treatment was applied for 10 minutes at 500°C based upon the anode preparation in other research groups [46],[47].

3.2.1.2 Electrolytes

The catholyte, later referred to as 1 M H_3PO_4/ 3 M KCl solution, was prepared by addition of 34 ml 85 wt% H_3PO_4, 101.1 gram of >99.5% KCl and 8.05 gram of >99.9% KOH. This mixture was carefully dissolved into MilliQ H_2O until a total of 500 ml of catholyte was produced. 500 ml of approximately 1 M H_3PO_4 was produced by addition of 34 ml 85 wt% H_3PO_4.

	pH	**Cond. [mS/cm]**
Catholyte	0.96	260.5
Anolyte	0.9	57.3

3.2.1.3 Ink compositions

The following materials were utilized for creation of the inks required. Sustainion XA-9 5% in Ethanol from Dioxide Materials, 60 wt% PTFE dispersion in H_2O from Sigma-Aldrich, 30-50nm PTFE NP by Nanoshel, Nafion 5 wt% 1100 W, IrO_2 NP 84.5% from Alta Aesar Premion, Cu NP <40 Nm. All inks have been sonicated for 30 minutes in an ice bath. Unless otherwise stated a hot-plate temperature of 85°C was used. The inks utilized are sorted based on their main ingredient. All 60wt% PTFE disp. layers have been treated in an oven at 250°C for 2 hours to remove a hydrophilic surfactant called Tergitol [74]. As is shown in Figure A.4 the heat treatment significantly increases the contact angle. The temperature of the treatment was chosen carefully at 250°C as to prevent any PTFE particles from sintering [56] and prevent possible degradation of Nafion at 280°C [53], from literature no definitive conclusion could be drawn on the influence of heat treatment on carbon paper. Surprisingly heat treatment at 350 °C, as was utilized in literature [74], was demonstrated to burn the samples and reduce the contact angle. For an equal comparison, PTFE NP layers without an additional ionomer have received a similar heat treatment.

Baselayers

PTFE Disp.: 30μL 60 wt% PTFE disp. was mixed with 3 ml MilliQ H_2O. To increase evaporation during spraycoating, the hot-plate was set to 110°C. After application of the layer a
PTFE NP: 40 mg PTFE was mixed with 4 ml isopropanol and 1 ml MilliQ H_2O. MilliQ H_2O was deemed unnecessary.

Catalyst layers

Cu: 20 mg Cu NP was mixed with 1 ml isopropanol, 1 ml MilliQ H_2O and 16 μL Nafion.
Cu/PTFE: 20 mg Cu Np mixed with 0.5 ml MilliQ H_2O and 0.3 ml isopropanol after which is was sonicated for 30 minutes in an ice bath. Secondly 7.5 mg PTFE NP, 0.5 ml isopropanol and 16 μL of Nafion was added to the copper ink. The finished ink was again sonicated for 30 min in an ice bath.

top layers

PTFE Disp.: 30μL 60 wt% PTFE disp. was mixed with 3 ml MilliQ H_2O. To increase evaporation during spraycoating, the hot-plate was set to 110°C.
PTFE NP: 40 mg PTFE was mixed with 4 ml isopropanol and 1 ml MilliQ H_2O. MilliQ H_2O was deemed unnecessary.
PTFE NP/ 2.5wt% Sustainion: 20 mg PTFE NP was mixed with 16 μL Sustainion.
PTFE NP/ 10wt% Sustainion: 20 mg PTFE NP was mixed with 2 ml isopropanol and 75 μL Sustainion.
PTFE NP/ 10wt% Nafion::20 mg PTFE NP was mixed with 2 ml isopropanol and 55 μL Nafion.

3.2.1.4 General set-up

All experiments were performed in a hybrid electrolyzer cell. A zero-gap configuration of a commercial membrane electrode assembly (MEA) CO_2 electrolyzer (Dioxide materials, T3 titanium anode current collector with a serpentine anolyte flow pattern and S3 stainless steel cathode current collector with a serpentine flow pattern and an active area of 5 cm^2) was modified by placing a custom made open catholyte flow field with a thickness of 3.4 mm was placed between the cathode and the membrane. The anode catalyst was pressed directly on to the membrane, to assemble the cell in a hybrid configuration. Tubing with an inner diameter of 1 mm connected the cell.

The gas-phase CO_2 feed rate was controlled by a mass flow controller (Bronkhorst F-201CV) and the cathode gas outlet flow rate was measured by a Bronkhorst F-101D type mass flow meter. 1 M H_3PO_4, 3 M KCl solution was used as the catholyte while a 1 M H_3PO_4 solution served as anolyte. Each was recirculated using a peristaltic pump (Longer BT100-1L, Darwin microfluidics). The cathode gas-phase product mixture was collected in the headspace of the sealed off catholyte reservoir and then fed into the in-line sampling loop of the gas chromatography (GC). The GC (Agilent 7890B) was equipped with a thermal conductivity detector (TCD) and a flame ionization detector (FID). A Molecular Sieve 3X column, SGE™ HT-8 0.25 µm capillary column, Hayesep Q packing (length 2.44 m) column, and Hayesep Q packing (length 0.5 m) column were used for the separation with argon as carrier gas. To determine the volume fraction of gas products in the cathode outlet. Liquid samples from the catholyte and anolyte were collected at the end of electrolysis and analyzed using high performance liquid chromatography (HPLC, Agilent 1260 infinity). The liquid sample was injected onto two Aminex HPX-87H columns (Biorad) connected in series and heated to a temperature of 60 °C. A 1 mM H_2SO_4 solution was used as eluent and a refractive index detector (RID) was used for the detection.

4

Catalyst stability

4.1. Experimental plan

As was shown in the initial tests, it is evident that the catalyst layer is unstable, either via undesired reactions of copper or physical detachment of particles. This lead to the following research question:

- Could a spray-coated Cu copper layer be stabilized within a highly acidic (pH=1) electrochemical cell?

To evaluate the stability of the catalyst layer in a highly acidic electrolyte and to investigate both the severity and underlying causes of this issue, a series of tests were conducted. This section is build up in the following sequence, following the performed experiments:

1. Determination of loss mechanism
2. Identification of main reactants
3. Evaluation of application of potential
4. Evaluation of alternative solutions

The first objective, distinguishing between mechanical or chemical deterioration resulted in straight forward tests as will be described. After determination of the loss mechanism the main reactants were observed via tests in alternating electrolytes. Lastly the devised solutions were verified and validated.

4.2. Test set-up

Two set-ups are created, the first method evaluates the detachment in a stationary bath of electrolyte, after each 3.75 minutes the GDE is transferred to another bath to mitigate possible diffusion limitations. The second evaluates the detachment of the catalyst layer within the regular flow cell set-up described in the general test set-up section with a flowing electrolyte (10.02 ml/min) and a CO_2 stream (15 sccm) applied via the GDE.
A total time of exposure of 15 minutes is maintained for both type of experiments. In case of a potential, chronopotentiometry was utilized and a current of 100 mA/cm^2 applied. At the end of the test, the cell was opened to air and samples of 0.3 ml were taken, diluted with 7.2 ml MilliQ water and tested. 20 ml of catholyte and anolyte were circulated through the system.
With exception of the tests regarding the loss mechanism all experiments are done via the second method. Additionally unless otherwise stated all catalyst layers have been applied via spray-coating and are 0.725 mg/cm^2 of Cu NP.
The copper quantity within the electrolyte is determined via Inductively Coupled Plasma Spectroscopy (ICP) measurements and is normalized by division of original loading, no distinction is made between metallic or dissolved copper in this manner. The ICP measurements represent a concentration of copper within the electrolyte, these results are normalized via the loading of the catalyst layer and are expressed by a percentage. Note that the percentage given does not provide any number of value as it is unknown to what ratio Cu_xO and metallic Cu were initially present within the catalyst layer. The number is merely a measure of deterioration of the catalyst layer.

4.3. Results and Analysis

4.3.1. Determination of the loss mechanism

Due to a lack of literature on catalyst layer detachment within CO_2 electrolysis the first step within this set of experiments is the determination of the loss mechanism. Especially distinguishing between mechanical, due to abrasive forces of electrolyte flow, and chemical detachment via reactions and subsequent dissolution of copper. Through comparison of detachment of the catalyst layer in stationary or flowing electrolyte as shown in Figure 4.1 a clear conclusion could be drawn that mechanical detachment is not the main mechanism present in the deterioration of the layer.

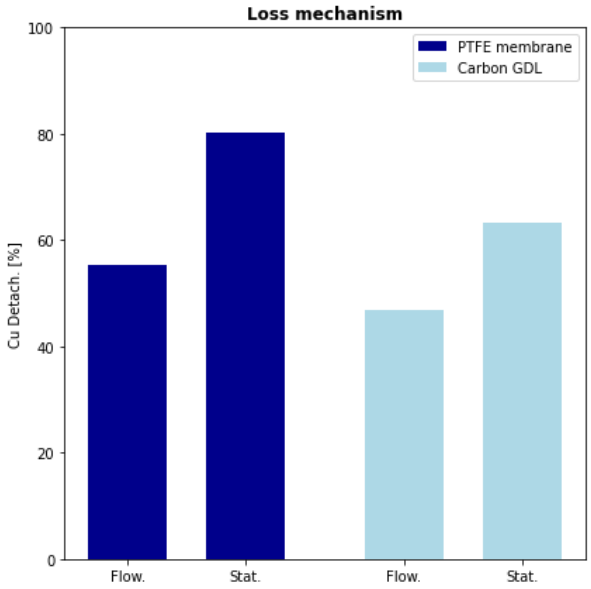

Figure 4.1: Influence of electrolyte flow on catalyst layer detachment.

4.3.2. Identification of reactants

Considering the chemical deterioration, five potential chemical paths have been identified from literature regarding multiple forms of copper. The ions required to dissolve Cu^{2+} such as Cl^- are not described in the equations as these do not act as reactants but rather as a catalyst, the Cl^- ions have a significant influence as these facilitate removal of reaction products via improved solubility of Copper [54]. Note that no caution has been taken regarding the reactions (ir-)reversibility and the signs presented.

1. [29]
$$2Cu + O_2 + 4H^+ \rightarrow 2Cu^{2+} + 2H_2O \tag{4.1}$$
2. [55]
$$Cu + 2H_2O \rightarrow Cu^{2+} + H_2 + 2OH^- \tag{4.2}$$
3. [19]
$$CuO + 2H^+ \rightarrow Cu^{2+} + H_2O \tag{4.3}$$
4. [48]
$$Cu_2O + 2H^+ \rightarrow Cu^{2+} + Cu + H_2O \tag{4.4}$$
5. [48]
$$2Cu_2O + 8H^+ + 2O_2 \rightarrow 2Cu^{2+} + 2H_2O \tag{4.5}$$

The above described reaction paths have been the foundation of the selection of electrolytes in the tests presented in Figure 4.2, as such providing a deeper insight into the deterioration mechanism of the catalyst layer.

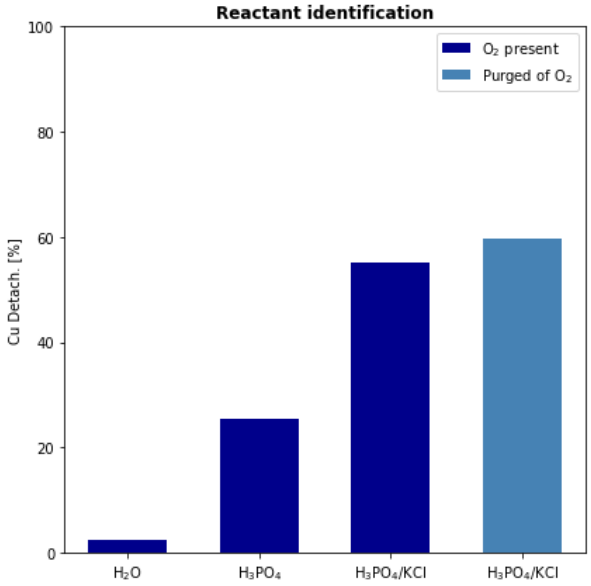

Figure 4.2: Influence of electrolyte on dissolution and catalyst layer detachment.

Referring to Figure 4.2, almost no detachment is observed in ultra-pure water while detachment increases with addition of phosphoric acid and KCl. It is clear that the main mechanism of catalyst loss is chemical.
Purging of the system with CO_2, thereby depriving the system of oxygen is found to be of no influence. This indicates that the first and fifth reaction proposed are not the most active deterioration mechanism. Additionally, the fourth reaction could be excluded as well. As stated in [19], the fifth reaction is far more aggressive then the fourth, as the fifth reaction is proven not to be the main cause of deterioration while in the presence of oxygen, the fourth reaction is excluded as well. The second reaction, or its variant including protons as reactant, is energetically unfavourable and non-spontaneous, only occuring within very rare conditions of very low concentration Cu^{2+} and hydrogen [55]. This leaves only the third reaction, a reaction confirmed to occur rapidly and within the time span of the experiment [19]. CuO was confirmed to be present on the catalyst layer via XRD as **SHOWN IN APPENDIX FIGURE:**

4.3.3. Evaluation of application of potential

After the identification of CuO dissolution to be the main mechanism through which the catalyst layer deteriorates. A solution was devised to apply a potential directly upon contact between electrolyte and catalyst layer. As can be seen in Figure 4.3, application of a current is shown to have a significant influence on the detachment of copper regardless of the electrolyte and detachment is nearly eliminated. These tests confirm that pure copper, the reduction product of copper-oxides, is stable within an acidic electrolyte.

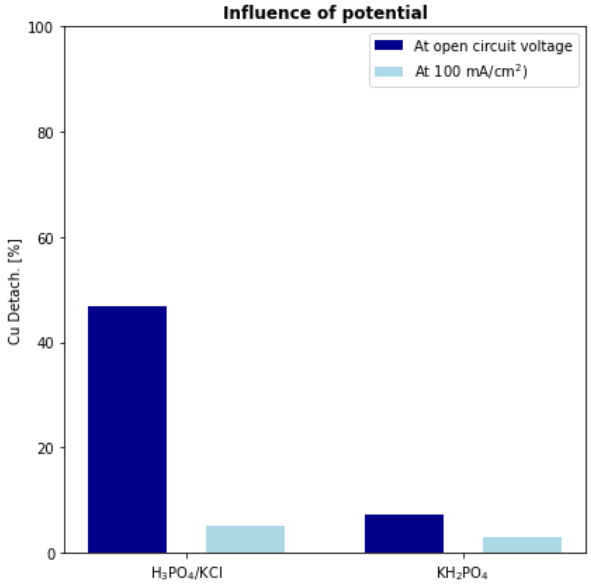

Figure 4.3: Influence of current density of 100 mA/cm2 on catalyst layer detachment in different electrolytes.

4.3.4. Evaluation of alternative solutions

As it is uncommon in CO_2 electrolysis to apply a potential directly when the electrolyte enters the catholyte flow chamber, multiple alternative paths have been tested on their effectiveness in Figure 4.4. The figure shows the solution or condition and the subsequent result on copper detachment compared to the base measurements.

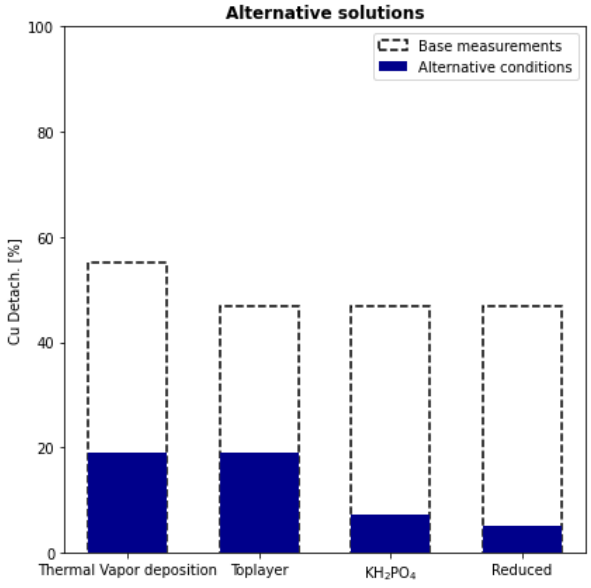

Figure 4.4: Alternative solutions to reduce deterioration of the catalyst layer.

The first alternative solution utilizes thermal vapor deposition instead of spray-coating to apply a very pure catalyst layer with limited amounts of copper oxides present. As shown this manner significantly reduces the amount of copper lost towards dissolution.
The second solution utilizes a highly hydrophobic PTFE-based top layer reducing the presence of electrolyte within the catalyst layer.
The third solution uses KH_2PO_4 as the starting electrolyte enabling a longer time before application of potential, being more in line with common practices in CO_2 electrolysis. Subsequent addition of a

mixture of concentrated potassium chloride and hydrochloric acid upon the start of the test would result in the desired electrolyte composition. Additionally this electrolyte would be a prime candidate for preliminary in-situ reduction of the catalyst layer to remove oxides.
Lastly a reduced catalyst layer has been tested on its stability. The catalyst layer was reduced in H_3PO_4/KCl and it was shown that although no potential was applied after an initial 15 minute reduction, a reduced catalyst layer cleared from copper oxides was comparably stable as when a constant potential was applied.

4.4. Summary and conclusion

The deterioration mechanism of copper has been identified to be primarily caused by chemical dissolution of CuO present on the nanoparticles. Multiple solutions have been tested, out of which reduction of the catalyst layer, either preliminary or during the experiment, has been found to be the most effective measure. Based on the foregoing chapter it has been decided to apply a potential directly upon contact between catalyst layer and electrolyte for the remainder of this project.
As a comparison with literature and examining Table A.2, it should be noted that most reported acidic cells either utilize a sputtered copper layer or a reduced copper layer [60].

5

Flooding tests

5.1. Experimental plan

As was described in chapter 3, the influence of PTFE based additives is of a large interest due to its strong hydrophobicity and low reactivity. The following research questions were proposed:

- How does a PTFE additive based layer on a sigracet 39BB GDL affect the flooding, voltage and FE within a highly acidic (pH=1) environment at a current density of 150 mA/cm^2?
- How does a PTFE additive based top layer influence the flooding, voltage and FE towards C2+ products in a highly acidic (pH=1) environment at a current density of 150 mA/cm^2?
- How does addition of PTFE NP within the catalyst layer affect the flooding, voltage and FE towards C2+ products in a highly acidic (pH=1) environment at a current density of 150 mA/cm^2?

In order to answer these questions a series of tests were devised in which multiple sets can be compared to examine the research questions. It should be noted that researchquestions regarding the different PTFE additives will partly be answered by the experiments in chapter 6. This section will be divided into three distinct subjects as per the questions above.

1. Flooding behaviour
2. Influences on potential
3. Faradaic efficiency

The following set of GDE's, as described in Table 5.1, were tested. Note that in all catalyst layers the quantity of copper is held constant, some GDE's have a mixed catalyst layer consisting of 0.725 mg/cm^2 Cu and 0.3 mg/cm^2 PTFE NP.

Base Layer [mg/cm^2]	Catalyst Layer [mg/cm^2]	Top Layer [mg/cm^2]
-	0.725 (Cu)	-
	0.725 (Cu) - (30% PTFE NP)	-
	0.725 (Cu)	0.25 (PTFE disp.)
	0.725 (Cu) - (30% PTFE NP)	0.25 (PTFE disp.)
0.5 (PTFE disp.)	0.725 (Cu)	-
	0.725 (Cu) - (30% PTFE NP)	-
	0.725 (Cu)	0.25 (PTFE disp.)
	0.725 (Cu) - (30% PTFE NP)	0.25 (PTFE disp.)
1.0 (PTFE disp.)	0.725 (Cu)	-
	0.725 (Cu) - (30% PTFE NP)	-
	0.725 (Cu)	0.25 (PTFE disp.)
	0.725 (Cu) - (30% PTFE NP)	0.25 (PTFE disp.)

Table 5.1: GDE compositions flooding tests

In order to assess the GDE's and their performance a current density of 150 mA/cm^2 was used. This current density was chosen based on the performance described by [60] and [76] which both showed product formation already at 150 mA/cm^2.

Within this section, firstly the proposed experiment and its results will be analysed after which an additional hypothesis is formulated on the flooding behaviour of these cells. The experimental set-up and its result will be highlighted shortly within section 5.5.

5.2. Test set-up

In order to quantify the flooding behaviour a method was adopted from [69]. The test utilized the general cell set-up as described above while boasting 15 sccm CO_2 and a flow rate of 10 ml/min. The alteration on the general cell set-up is as follows. An additional beaker placed upon a scale was positioned between the cathodic gaseous outlet tube and the cathodic catholyte beaker, the connection between the cell and the weighed beaker was a 4 mm diameter tube. The beaker collects the flooded catholyte and was quantified via the scale. A constant current density of 150 mA/cm^2 was applied for all tests. 40 ml of catholyte and anolyte were circulated through the cell, note that due to the quantity of the catholyte there is a maximum amount of flooding, the tests are stopped after this amount is reached. The cathodic effluent gasses were analyzed for products every 10 minutes via the GC.

5.3. Results

5.3.1. Flooding behaviour

The flooding behaviour of the set of 12 GDE's have been graphically depicted in the figure below.

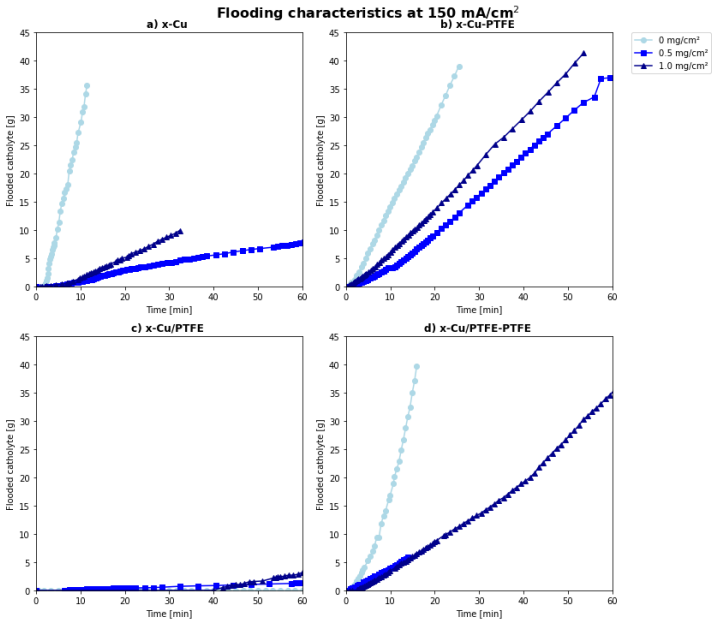

Figure 5.1: Flooding behaviour as a function of PTFE base-layer thickness with various types of catalyst layers **a)** Catalyst layer consisting of Cu NP only **b)** Catalyst layer consisting of Cu NP and a PTFE Top layer **c)** Catalyst layer consisting of a 70/30% mix of Cu NP an PTFE NP. **d)** Catalyst layer consisting of a 70/30% mix of Cu NP an PTFE NP and a PTFE Top layer.

The first trend to be recognised is the large influence of a PTFE top layer, graphically depicted in Figure 5.1b and d. Surprisingly a PTFE top layer induces flooding even though hydrophobic material has been added.
The second trend to be recognised is the large difference between GDE's with a copper catalyst layer compared to a copper/PTFE catalyst layer. A severe reduction of flooding is observed. It should be noted that this trend is insignificant in the case of application of a PTFE top layer.
The third trend to be observed is the large influence of the applied base layer of PTFE, however no

significant relation is found between the thickness of the baselayer and the flooding rate.

5.3.2. Influences on potential

Chronoamperometric curves at 150 mA/cm^2 have been summarized in Figure 5.2. The first 5 minutes have been presented as to highlight the specific shapes.

Figure 5.2: Chronopotentiometric curves for different catalyst layer composition and base layer thickness **a)** Catalyst layer consisting of Cu NPs only **b)** Catalyst layer consisting of a 70/30% mix of Cu NPs and PTFE NPs. **c)** Catalyst layer consisting of Cu NPs and a PTFE Top layer **d)** Catalyst layer consisting of a 70/30% mix of Cu NPs and PTFE NPs and a PTFE Top layer.

From the figure a surprising sinusoidal pattern can be observed on the recorded potentials of GDE's with top layers as shown in Figure 5.2c and d. The GDE's with a mixed catalyst layer also show a periodic pattern but with a far larger period. These described periods are caused by the formation of bubbles on the catalyst layer, these bubbles temporarily reduce the amount of active sites leading to the increase in voltage.
Considering the impact of the baselayer on the required potential no significant impact was discovered as is shown in Table 5.2. Although the average potential of all four types of layers increased with increasing baselayer thickness, the pattern was believed to be too insignificant and it was concluded that another more decisive factor must be at play.
A pattern was observed considering the influence of addition of a top layer, considering all 6 cell combinations of base and catalyst layer, shown in the second and third column of Table 5.2, an increase in average voltage was noted after addition of a top layer.
Considering the utilization of PTFE NP, a minor pattern was observed, with 5 out of 6 comparisons showing a higher potential after addition.

Baselayer	X-Cu	X-Cu/PTFE	X-Cu-PTFE	X-Cu/PTFE-PTFE	AVG
-	3.72 V	4.15 V	3.86 V	4.78 V	4.13
0.5	4.05 V	4.10 V	4.65 V	4.25 V	4.26
1	4.17 V	4.18 V	4.2 V	4.65 V	4.3
AVG	3.98 V	4.14 V	4.24 V	4.55 V	-

Table 5.2: Average potentials recorded on 150 mA/cm^2, sorted on baselayer thickness

5.3.3. Faradaic efficiency

The faradaic performance of each GDE is depicted in Figure 5.3. It should be noted that due to the set-up, the system as a whole has large volume, the reported FE's towards gaseous products are therefore significantly skewered compared to tests done using the general set-up.

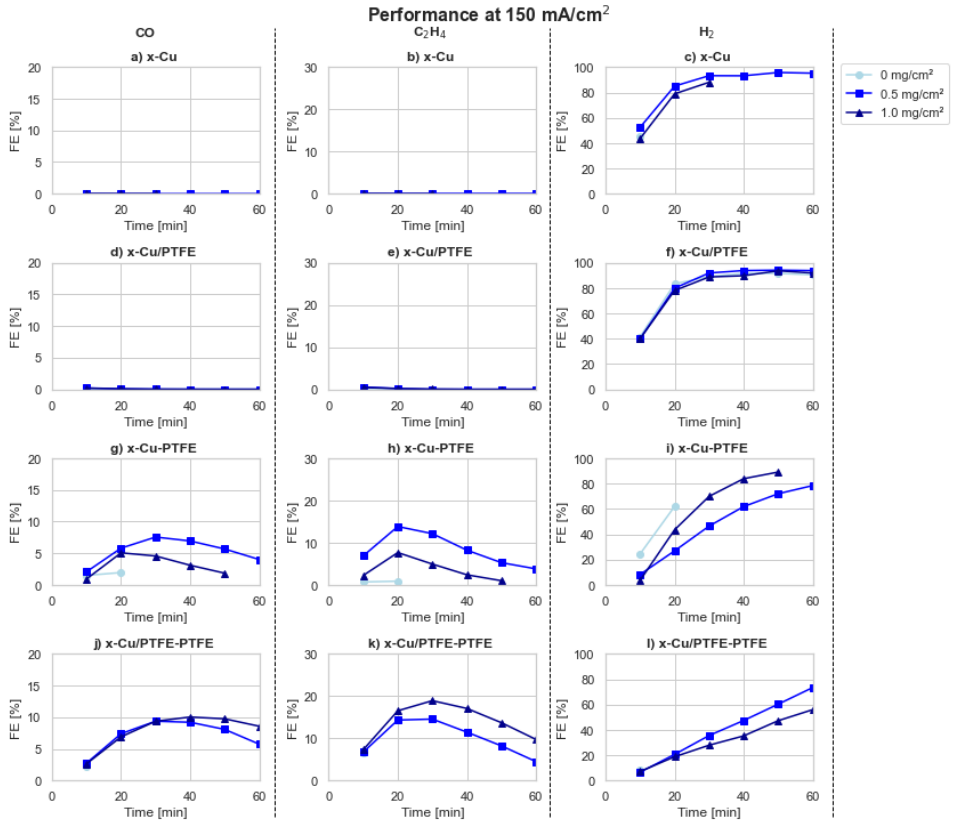

Figure 5.3: Faradaic efficiency of H2, C2H4 and CO as a function of time for different catalyst layer archetypes and base layer thicknesses. The left column showing the FE towards CO, the middle column towards C2H4 FE and the right column towards H_2. **a-c)** The catalyst layer consisting of Cu NPs, **d-f)** the catalyst layer consisting of a 70/30% mix of Cu NPs and PTFE NPs. **g-i)** Catalyst layer consisting of Cu NP and a PTFE Top layer **j-l**) Catalyst layer consisting of a 70/30% mix of Cu NP an PTFE NP and a PTFE Top layer.

As is clearly seen in the figure, the top layer enables a faradaic efficiency towards C- products whereas GDE's without all produce only hydrogen.
The presence of PTFE NP has a positive and significant effect on the production of C- products as both comparison of Figure 5.3a-c and d-f, and comparison of g-i and j-l show a significant improvement in C- product formation.
The influence of the baselayer is harder to determine due to the flooding of cells without baselayer resulting in abortion of the experiment. However, looking at top layer containing GDE's only, the performance of a mixed catalyst layer is shown to be equal for the first 20 minutes, the performance of the copper based layer was far below. No significant conclusion can be drawn on the influence of a baselayer on the FE.

A last thing to be noted is the low stability of the cells, all show a significant production of C- products at the start of the experiment after which a fast reduction takes place producing limiting amounts of products near the end of the experiment.

5.4. Analysis

An interesting phenomenon regarding the flooding was observed and to be highlighted in this section. As was noticed within the potential curves two distinct periodic patterns were observed comparing the Cu/PTFE and the top layer containing archetypes. This was concluded to be due to gas presence within the catalyst layer and as such was believed to be related with bubble detachment behaviour. As could be seen in Figure 5.1, the PTFE top layer was actually shown to induce flooding and a hypothesis was formed on the connection between the potential curves and the flooding behaviour.

- The flooding behaviour is connected to bubble detachment via an induced capillary pressure within the catholyte outlet tube.

The capillary pressure within a mixed phase column is related to the surface area, a higher amount of smaller bubbles therefore create an additional capillary pressure. The capillary pressure within a tube is also strongly related to the tube diameter and thus an additional experiment was proposed.

5.5. Influence of catholyte outlet tube diameter

As stated the basis of this experiment is to examine the influence of tube diameter on flooding behaviour of a GDE with a top layer.
The test set-up was similar as described in section 5.2 with the exception of the catholyte outlet tube diameter being increased from 1 mm to 4 mm in diameter.

In the figure below the influence on flooding behaviour, the potential and faradaic efficiency have been summarized for two catalyst layer archetypes with top layers, on the left without and on the right with a baselayer.

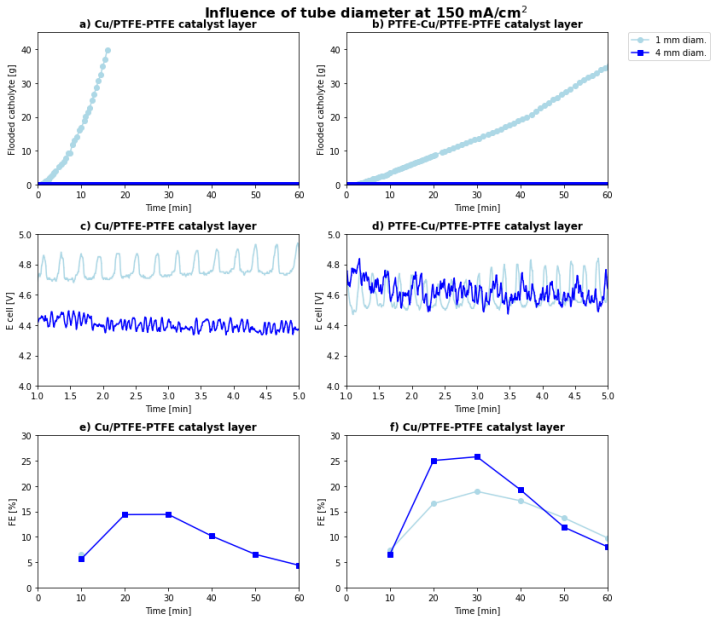

Figure 5.4: Influence of the catholyte tube diameter on **a,b)** flooding rate and **c,d)** cell potential and **e,f)** FE towards ethylene.

The widened tube resolved the flooding behaviour of the cell and additionally altered the potential pattern and reduced its periodicity. Validating the hypothesis of a relation between the tube diameter, flooding and potential curves. The faradaic efficiency is suggested to increase as well upon substitution, this might be due to the reduced pressure variations caused by the capillary pressure.

5.6. Summary and conclusion

Regarding the sub-questions of interest within this chapter the following conclusions can be drawn.

- How does a PTFE additive based layer on a sigracet 39BB GDL affect the flooding, voltage and FE within a highly acidic (pH=1) environment at a current density of 150 mA/cm^2?
- How does a PTFE additive based top layer influence the flooding, voltage and FE towards C2+ products in a highly acidic (pH=1) environment at a current density of 150 mA/cm^2?
- How does addition of PTFE NP within the catalyst layer affect the flooding, voltage and FE towards C2+ products in a highly acidic (pH=1) environment at a current density of 150 mA/cm^2?

A PTFE dispersion based baselayer has a significant effect on the flooding behaviour of the cell, while no significant distinction could be made on the influence of the thickness of the baselayer regarding flooding. Regardless, a more elegant and simple manner has been identified via the increment of the catholyte outlet tube diameter. This will therefore be the approach of choice within the remainder of this project. Considering the influence of a PTFE dispersion base layer on voltage and FE limited answers could be provided due to flooding behaviour stopping the cell. The potential is suggested to be effected by the addition and thickness of a baselayer although an unknown factor seems to have a larger influence. As for evaluation of the Faradaic efficiency, Figure 5.4e and f, especially the ”4mm diam” class, could be used for comparison and analysis of the influence of the baselayer. It shows a significant advantage due to a PTFE baselayer.

Considering sub-question 2 a clear influence on flooding was observed, this was found due to the influence of the top layer on the bubbles. The potential showed a clear pattern, comparison of cells with and without a top layer shows that the average potential is higher for each composition used. The faradaic efficiency was positively influenced by the top layer.

Lastly considering sub-question 3 a clear reduction of flooding was observed within the sample class without top layer, this pattern was not extended towards the archetypes with a top layer. The voltage again showed a minor correlation with the addition of PTFE NP within the catalyst layer. A clear enhancement of performance was observed and PTFE NP will remain within the catalyst layer for the remainder of this project.

6

CO_2R tests

6.1. Experimental plan

As was discussed in the chapter 6, the answer on the two research questions regarding the influence of PTFE additives required an additional set of experiments before an answer could be formulated. Within this chapter, the flooding free set-up will designed in the last chapter will be utilized to give a final answer on the four research questions stated below. Note that flooding is no longer a metric of interest.

- How does a PTFE additive based layer on a sigracet 39BB GDL affect the flooding properties and voltage within a highly acidic (pH=1) environment at a current density of 150 mA/cm^2?
- How does a PTFE additive based top layer influence the flooding, voltage and FE towards C2+ products in a highly acidic (pH=1) environment at a current density of 150 mA/cm^2?
- How does an increased current density affect the FE towards C2+ products in a highly acidic (pH=1) environment at a current density of 150 mA/cm^2?

A more complete answer on these sub-questions will be the result of the tests inspired by the set of experiments within this section.

An additional research question was formulated regarding the stability issues faced within the last chapter.

- What are the main causes of performance instability of a Sigracet 39BB based cell with a PTFE based baselayer, Cu/PTFE catalyst layer and a PTFE disp. top layer and how can the stability be improved?

Microscopic examination of a sample yielded the following pictures.

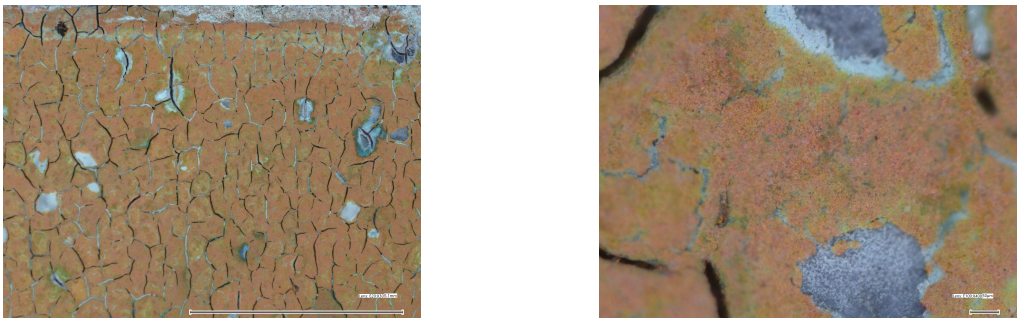

(a) (b)

Figure 6.1: Microscopic imagery **a) 20X, b) 400X**of GDE with PTFE disp. top layer after 1 hour of electrolysis at 150 mA/cm^2 in strong acid

Exposed copper would yield hydrogen as proven in chapter 5, top layer detachment as is shown to be present could therefore be the cause of the instability observed.

Considering the additional research question regarding stability, three hypotheses were formed:

1. The top layer is destabilized due to a lack of mechanical stability
This hypothesis is based upon the microscopic pictures in Figure 6.1, a proposed solution is to increase the amount of PTFE disp. thereby possibly mechanically enforcing the top layer. The following GDE's were produced.

Baselayer [mg/cm]	Catalyst layer	Top layer
1.0 (PTFE disp.)	0.725 (Cu) - (30% PTFE NP)	0.25 (PTFE disp.)
1.0 (PTFE disp.)	0.725 (Cu) - (30% PTFE NP)	0.5 (PTFE disp.)
1.0 (PTFE disp.)	0.725 (Cu) - (30% PTFE NP)	1 (PTFE disp.)

Table 6.1: GDE's produced to determine the influence of top layer thickness on stability

2. The top layer is destabilized by the entrapment of water within the catalyst layer.
As described in [76] it is important for a top layer to support both water and gas transport through the top layer. As this strongly hydrophobic layer is expected to allow limited water transport, Water transport might have to be increased to stabilize the top layer. This was approached in two manners: via the use of PTFE NP as top layer, and by addition of an anion exchange ionomer boasting both local hydrophilicity and proton adversion. Note that this set of tests also yields a more complete answer on the second sub questions regarding PTFE additives as a top layer.

Baselayer [mg/cm]	Catalyst layer	Top layer
1.0 (PTFE disp.)	0.725 (Cu) - (30% PTFE NP)	0.25 (PTFE NP)
1.0 (PTFE disp.)	0.725 (Cu) - (30% PTFE NP)	0.6 (PTFE NP) - 2.5% Sust.
1.0 (PTFE disp.)	0.725 (Cu) - (30% PTFE NP)	0.6 (PTFE NP) - 10% Sust.
1.0 (PTFE disp.)	0.725 (Cu) - (30% PTFE NP)	0.6 (PTFE NP) - 10% Naf.

Table 6.2: PTFE NP based adlayes

3. The top layer is destabilized by hydrogen formation on exposed copper and or carbon sites within the cracks of the substrate.
As could be observed in Figure 6.1a, most top layer defects surround large cracks within the carbon substrate. As stated before, exposed copper or carbon will result in vigorous HER. By application of PTFE NP as baselayer, the cracks of the substrate could partially be filled reducing their influence.

Baselayer [mg/cm]	Catalyst layer	Top layer
1.0 (PTFE NP)	0.725 (Cu) - (30% PTFE NP)	0.25 (PTFE disp.)

Table 6.3: GDE composition boasting a PTFE NP baselayer

Additionally, a comparison with acidic cells in literature show the majority to be utilizing a PTFE membrane [23] [76] or a custom PTFE based layer [74]. Therefore a logical approach would be to mimic these reports as is attempted via this hypothesis.

6.2. Test set-up

The test set-up used for the CO_2R tests are as described in subsubsection 3.2.1.4. 40 ml of catholyte and anolyte were used of similar composition as described. 15 sccm of CO_2 is supplied towards the cathode while 10 ml/min of catholyte and anolyte circulates through the cell. A 4 mm diameter tube was used as catholyte outlet tube. The cathodic effluent gasses were analyzed for products every 10 minutes via the GC.

6.3. Results and Analysis

6.3.1. Hypothesis 1

The results of the set of experiments described are summarized the figure below.

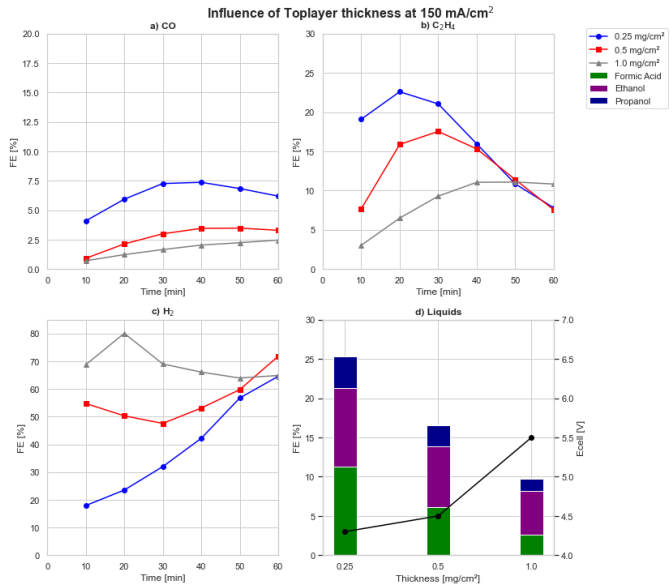

Figure 6.2: Influence of an increased PTFE disp. toplayer thickness on the FE and voltage at 150 mA/cm^2. **a)** FE of CO, **b)** FE of C_2H_4, **c)** FE of H_2 and **d)** FE towards liquid products and cell voltage.

A clear trend is observed regarding the performance of the cells, as the top layer thickens the FE towards C- products decreases. It should be noted however that the performance of the thickest top layer shows a more stable trend regarding both CO and C_2H_4. Microscopic pictures after the tests showed no visually significant trend in the top layer surface, all showed signs of damage. Additionally the voltage is shown to increase with an increasing toplayer thickness.

6.3.2. Hypothesis 2

The PTFE NP based top layers as described in Table 6.1 yielded the results depicted in Figure 6.3.

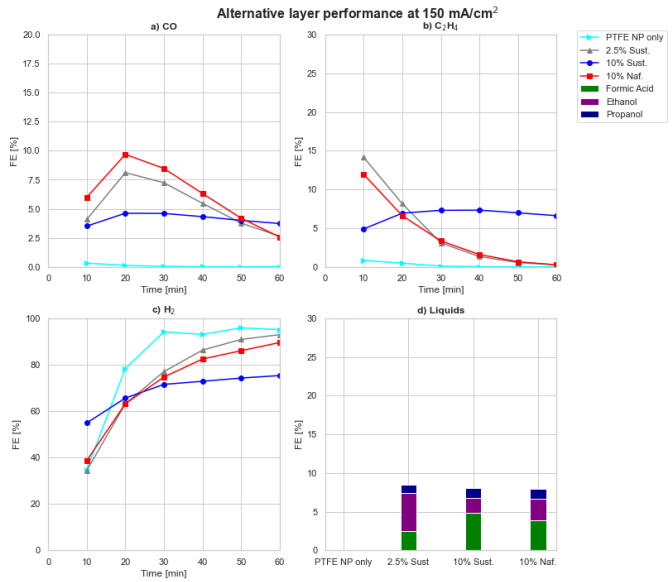

Figure 6.3: Electrochemical CO_2 reduction performance of a number of PTFE NP based toplayers. FEs of the generated products at 150 mA/cm2 as a function of time, **a)** FE of CO, **b)** FE of C_2H_4, **c)** FE of H_2 **d)** FE towards liquid

Important to notice is the comparison between a PTFE NP based top layer compared to the PTFE disp. based top layer. The PTFE NP based top layer showed no stability whatsoever and acted similar to a Cu/PTFE cell as described in Figure 5.3. The samples were treated exactly the same including oven treatment, this highlights a significant difference between the two types of additives. Although it is unclear if this is due to the surfactant, particle size or any other unknown compound within the dispersion, a conclusion can be drawn on the solo use of the selected PTFE additives as a top layer. The ionomers added stability to the PTFE NP with different outcomes. As can be deduced the more hydrophobic samples had a significantly higher initial yield then the high concentration sustainion based PTFE NP top layer, supporting the requirement for hydrophobicity in the top layer as discussed in subsubsection 2.4.3.2. The stability is however increased with an increasing amount of sustainion although with a low performance, it is unclear how this mechanism works.

6.3.3. Hypothesis 3

As is shown via the microscopic pictures in Figure 6.4 a clear difference could be observed for the base layer surface of the GDL. As was hypothesised the cracks are notably altered resulting potentially in a more homogeneous base layer with less exposed carbon and copper sites.

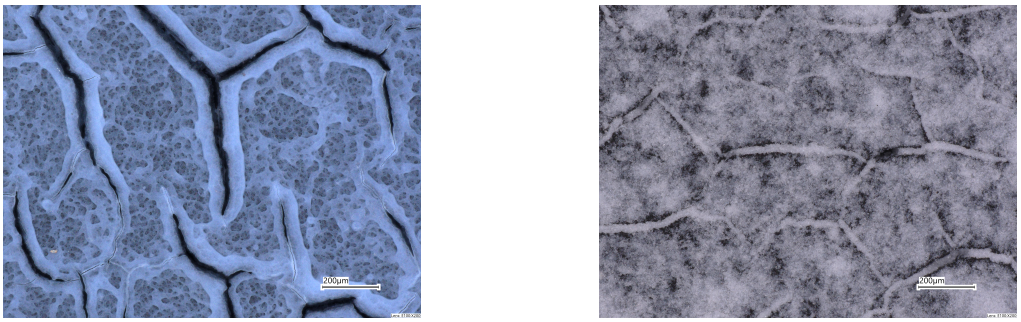

(a) **(b)**

Figure 6.4: Microscopic imagery **a)** PTFE NP baselayer (200X), **b)** PTFE disp. baselayer (200X)

The effect of this alteration of the baselayer on the stability is large as can be concluded from Figure 6.5a, at higher current densities the stability is shown to decay slightly. The Figure 6.5b is a more graphical depiction of the results including the C2+ product formation. A clear trend, as supported by literature, is found for increment of the current density.

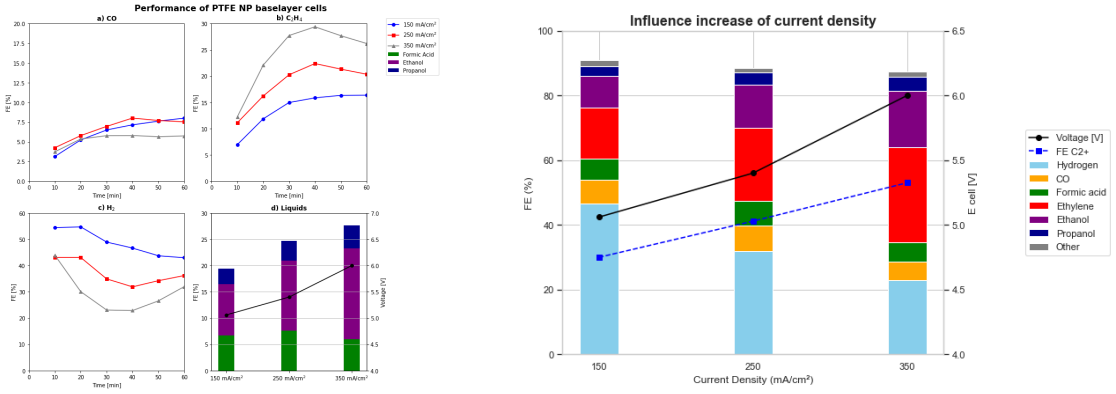

(a) **(b)**

Figure 6.5: Influence of the current density on CO_2 reduction efficiency and product selectivity. Faradaic efficiency of the generated products at three different current densities with 15 sccm CO_2, 1 M H_3PO_4/KCl catholyte and 1 M H_3PO_4 anolyte on PTFE NP based layer. **a)** Stability of performance, **b)** Graphical depiction of results after 40 minutes including C2+ product formation

Additionally an increased initial HER activity was measured although it was expected that a reduced

amount of exposed copper and carbon sites would, along with increasing the stability of the top layer, reduce the amount of hydrogen produced. In contradiction with the implied consequences of the hypothesis tested, actually the initial hydrogen yield is significantly higher compared to experiments utilizing the PTFE dispersion based base layer. This comparison will be examined in more depth in chapter 7.

At the highest current density, after 40 minutes, the cell boasted a FE towards C2+ products of 53%. A FE of 29.4% towards ethylene was reached and on average over the course of an hour an FE of 17.3% was realized towards ethanol, additionally 4.3% of the electrons went towards propanol production.

Microscopic inspection of the GDE's show minimal damage to the top layer. The white color and the blue crystals are explained by insufficient rinsing and are believed to be KCl.

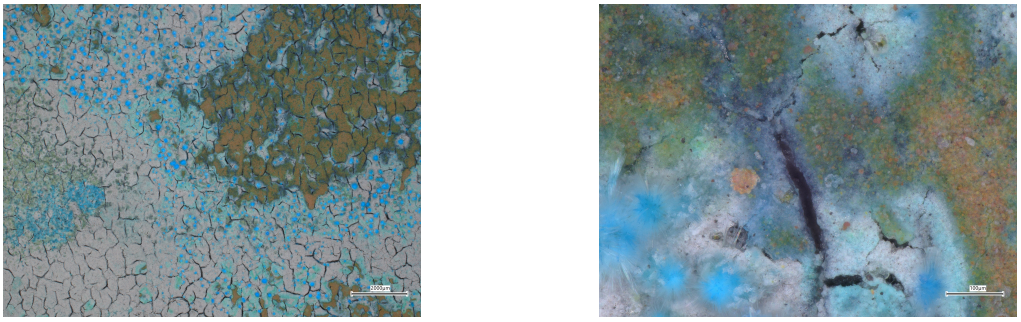

(a) **(b)**

Figure 6.6: Microscopic imagery **a) 20X, b) 400X**of GDE with PTFE disp. top layer after 1 hour of electrolysis at 150 mA/cm^2 in strong acid

6.4. Summary and conclusion

As is described in the analysis a path was founds towards stability answering the additional sub-question. As shown in subsection 6.3.3, utilization of a PTFE NP based base layer has shown clear advantages compared to the use of 60% PTFE dispersion considering stability of the cell. This is theorized to be primarily due to the reduced size of the cracks reducing exposed copper or carbon sites. Additionally the potential required was significantly higher then the PTFE dispersion variant, supporting the reduction of exposed copper and carbon sites. It is clear that the cracks embedded in the Sigracet 39BB substrate exert a large influence on the stability of the cell.

Regarding the initial sub-questions, the experiments conducted have shown a more complete answer.

- How does a PTFE additive based layer on a sigracet 39BB GDL affect the flooding, voltage and FE within a highly acidic (pH=1) environment at a current density of 150 mA/cm^2?
- How does a PTFE additive based top layer influence the flooding, voltage and FE towards C2+ products in a highly acidic (pH=1) environment at a current density of 150 mA/cm^2?
- How does an increased current density affect the FE towards C2+ products in a highly acidic (pH=1) environment?

Upon the first sub-question a more complete answer is given in the data provided by subsection 6.3.3 by the tests regarding the second additive, PTFE NP. Considering the FE an increase was found primarily due to an increased stability, the initial performance was reduced upon substitution. The voltage as is shown in Figure 7.1 was increased.
Regarding the second sub-question addressed in this chapter, it is found that PTFE NP are less stable compared to the PTFE dispersion and thereby yield a reduced performance, likely due to a difference in mechanical stability. It is unknown what compound within the PTFE dispersion is to be associated with this increased mechanical stability. A PTFE NP top layer could be used in combination with ionomers and it is shown that hydrophobic Nafion is preferred as is supported by the analysis in chapter 2. However comparison between the use of PTFE NP and PTFE disp. as a top layer yields a strong preference

towards the use of PTFE dispersion, based on both the performance and the stability of the top layer. Regarding the third sub-question a clear trend was observed and current density significantly increased the performance of acidic cells as expected through the literature review.

7

Discussion

Within the following section the conclusions drawn on the researchquestions shall be presented.

The following research question was assessed via literature study.

What is the optimal configuration in terms of electrode, catalyst and electrolyte for direct CO_2 electrolysis towards high energy density liquids with minimal downstream process?

This research question was evaluated along the following two sub-questions.

- What is the performance of current state of the art CO_2 electrolysers towards liquid products, and what liquid product is currently the most optimal goal product?
- What are the design distinct downstream processes associated with CO_2R towards liquid products?

As is elaborately explained in chapter 2, the optimal target product was found to be ethanol based on the relatively high maturity of CO2R towards ethanol, its high HHV and the relatively valuable yield per electron. The optimal cell configuration was subsequently determined mainly on two key parameters towards industrialization. The CO_2 conversion rate and the potential for ethanol extraction, both reducing the need for downstream processes. Optimizing towards these parameters led to the design of a highly acidic cell of configuration number 3 boasting a mature Nafion 117 membrane, high CO_2 conversion rate and a high potential stability and ethanol concentration.

Within the remainder of this report, experimental work was performed towards the design of such a cell. A sigracet 39BB carbon paper was used as GDL to omit conductivity problems of PTFE membrane.
This lead to the following main research questions regarding the design of this cell.

Could a regular commercially bought carbon based GDE with 0.7 mg/cm^2 Cu and an area of 5 cm^2, be modified for CO_2 reduction towards C2+ products with a Faradaic efficiency above 40% in highly acidic conditions via hydrophobification by addition of PTFE beneath, within or on top of the catalyst layer?

Along with the following sub-questions the answer of which will be described in the remainder of this section.

- Could a spray-coated Cu copper layer be stabilized within a highly acidic (pH=1) electrochemical cell?
- How does a PTFE additive based layer on a sigracet 39BB GDL affect the flooding, voltage and FE within a highly acidic (pH=1) environment at a current density of 150 mA/cm^2?
- How does a PTFE additive based top layer influence the flooding, voltage and FE towards C2+ products in a highly acidic (pH=1) environment at a current density of 150 mA/cm^2?

- How does addition of PTFE NP within the catalyst layer affect the flooding, voltage and FE towards C2+ products in a highly acidic (pH=1) environment at a current density of 150 mA/cm^2?
- How does an increased current density affect the FE towards C2+ products in a highly acidic (pH=1) environment?
- What are the main causes of performance instability of a Sigracet 39BB based cell with a PTFE based baselayer, Cu/PTFE catalyst layer and a PTFE disp. top layer and how can the stability be improved?

Could a spray-coated Cu copper layer be stabilized within a highly acidic (pH=1) electrochemical cell?
As was described in chapter 4, the presence of a strong acid in combination with a high concentration of KCl could significantly deteriorate the catalyst layer. The culprit was identified to be the dissolution of CuO, a process which could be stopped via the application of a potential. Other solutions included preliminary reduction of CuO towards Cu or the use of alternative techniques of catalyst layer application yielding copper layers with a lower amount of CuO. Comparison with literature showed that reports utilizing copper in a similar environment all, possibly without realizing opted for one of the mentioned solutions.

How does a PTFE additive based base layer on a sigracet 39BB GDL affect the flooding, voltage and FE within a highly acidic (pH=1) environment at a current density of 150 mA/cm^2?
Two PTFE based additives were utilized as a base layer to improve the hydrophobicity of a Sigracet 39BB GDL. Considering flooding an improvement was made utilizing a PTFE dispersion based layer, however a more elegant solution was determined omitting the need for flood reduction in acidic cells. Additionally only a weak correlation between the required potential for 150 mA/cm^2 and the thickness of the PTFE dispersion layer was observed. Lastly the faradaic performance was shown to improve significantly, even when flooding was no longer an issue, corresponding to the results of [3] which took a similar approach of increasing the hydrophobicity of the substrate.

Comparison between the two PTFE additives, PTFE dispersion and PTFE NP, is done in the figure below. Each of the two GDE's consist of a sigracet 39BB substrate with a 1 mg/cm^2 heattreated baselayer, a Cu/PTFE catalyst layer and a 0.25 mg/cm^2 PTFE dispersion top layer.

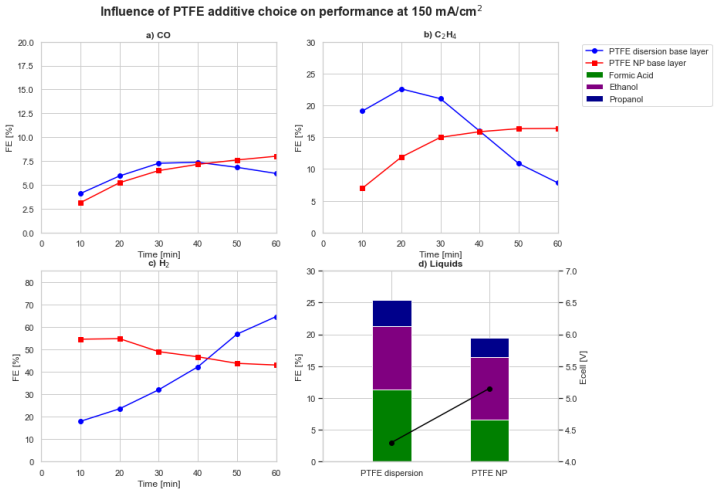

Figure 7.1: Performance of two GDE's with a different PTFE additive utilized as base layer. At 150 mA/cm^2 and 15 SCCM of CO_2 feed

A number of trends are observed, considering the stability of C2+ product formation it is clear that the PTFE NP based base layer yields a more stable production, each of the products seemingly approaching an asymptote over the course of an hour. As opposed to the PTFE disp. based base layer which showed significant deterioration, however, the initial formation of products is significantly higher. Even if compared to the performance of PTFE NP based cells at 350 mA/cm^2 the first measurement of

ethylene after 10 minutes is higher. This suggests an incredibly high initial performance for the PTFE dispersion based cells above 30% towards C_2H_4. On average the faradaic efficiency of ethanol was shown to be equal for both types.

The voltage is shown to be significantly higher for the PTFE NP base layer supporting the theory that exposed copper or carbon sites are reduced due to the substitution of PTFE additive. A fluke could be ruled out by looking at the voltages reported in Table 5.2 and Figure 6.5b.

Combining these datapoints a theory is formulated on the role of the cracks of the substrate within the PTFE disp. based cells. Evaluating hypothesis 3, the theorized reduced amount of exposed copper and carbon sites is supported by comparison of the potential required. However the performance seems to point another way as hydrogen formation was associated with exposed copper or carbon sites.

It is hypothesized that mass transfer of CO_2 towards the catalyst layer is reduced due to application of a PTFE NP base layer. A similar principle was found in literature [69], the study cited infiltrated PTFE particles into the cracks of a GDL leading to a slightly reduced CO_2 permeation. It should be noted that the effects attributed to the reduced CO_2 permeance were severly limited compared to the observed decline in performance within this report. Testing the CO_2 permeance as was done in the report cited above would be a logical step to evaluate the hypothesis.

How does a PTFE additive based top layer influence the flooding, voltage and FE towards C2+ products in a highly acidic (pH=1) environment at a current density of 150 mA/cm^2?
A PTFE based additive has succesfully been applied as a top layer to increase performance towards C2+ products in acidic environment. Coinciding with the analysis within subsubsection 2.4.3.2, the hydrophobicity of the PTFE dispersion showed a significant increment of performance towards C2 products.
Both PTFE disp. and PTFE NP showed a decreasing trend regarding performance, in case of PTFE NP this decline was shown to be far faster indicating a faster decay of the top layer. It was observed that an ionomer slightly stabilizes the PTFE NP, however the top layer was not nearly as stable as with using PTFE dispersion. Increasing the amount of Sustainion increased the stability but its hydrophilicity was theorized to limit the performance of the cell.

In the end the author identified a 0.25 mg/cm^2 top layer of PTFE dispersion to be the most optimal, thicker layers were found to reduce performance. A significant trend was observed regarding the influence of a PTFE top layer on the potential of the cell as was discussed earlier in chapter 5. Additionally a positive correlation was observed after setting out the potential against the thickness of the top layer. Lastly, flooding was surprisingly observed to be caused by the top layer due to its influence on the bubbling behaviour of the GDE, this problem was resolved by application of a thicker catholyte outlet tube to reduce the induced capillary pressure.

How does addition of PTFE NP within the catalyst layer affect the flooding, voltage and FE towards C2+ products in a highly acidic (pH=1) environment at a current density of 150 mA/cm^2?
Results showed a significant improvement of faradaic efficiency upon addition of 30% PTFE NP within the catalyst layer as was proven for other conditions within literature [71], [4]. Additionally flooding was severely reduced within the catalyst layer archetypes lacking a top layer. Again no significant trend regarding the voltage was observed although a weak correlation was noticed.

How does an increased current density affect the FE towards C2+ products in a highly acidic (pH=1) environment?
As could be expected from literature a significant improvement of faradaic efficiency, improving from a total faradaic efficiency towards C2+ products of 30.5% towards a total C2+ faradaic efficiency of 53.0% of which 29.4% towards ethylene, 17.3 % towards ethanol and 4.3 % towards propanol. An additional 2% went towards acetic acid, ethylene glycol and propionaldehyde.

What are the main causes of performance instability of a Sigracet 39BB based cell with a PTFE based baselayer, Cu/PTFE catalyst layer and a PTFE disp. top layer and how can the stability be improved?
The main cause of performance instability is believed to be due to the cracks in the carbon substrate. Reduction of the cracks by application of 1 mg/cm^2 PTFE NP showed a severe increase in stability of these cells. Exposed carbon and or copper were believed to be the culprit for the lack in stability. A stability of at least an hour was achieved on 150 mA/cm^2 in this manner. This result strongly suggests the use of PTFE membrane as a substrate as is common within acidic electrolysis.

Could a regular commercially bought carbon based GDE with 0.7 mg/cm^2 Cu and an area of 5 cm^2, be modified for CO_2 reduction towards C2+ products with a Faradaic efficiency above 40% in highly acidic conditions via hydrophobification by addition of PTFE beneath, within or on top of the catalyst layer?
The main research question could, in light of the results, be answered with a simple 'Yes', a regular sigracet 39BB carbon paper was successfully modified by a multitude of PTFE additions; beneath, within and on top of the catalyst layers. It was shown that all PTFE has a positive influence on C2+ formation in every possible position relative to the catalyst layer, with the largest influence attributed to the top layer. The goal of 40% towards C2+ products was surpassed and a very respectable faradaic efficiency was achieved.

8

Conclusions and recommendations

Within this report an assessment was made on the feasibility towards industrial scale application, which led to the design and build of a cell operating within a highly acidic environment of type 3 as described in Figure 2.2. A multitude of solutions were found before reaching to the final results. Catalyst layer deterioration was omitted via the direct application of potential upon contact with the electrolyte as to reduce possible copper oxides, preventing their dissolution. Flooding of the GDE was demonstrated to be due to a capillary pressure build up in the catholyte output tube. A modified catholyte tube with a diameter of 4 mm as opposed to an initial 1 mm was shown to prevent flooding.
The design modified a Sigracet 39BB substrate with PTFE allowing for significant C product formation. Two types of PTFE additives were used beneath, within and on top of the traditional catalyst layer, addition of PTFE on all three positions was found to be beneficial towards the formation of C2+ products.

Considering the baselayer, addition of PTFE dispersion was shown to have a clear and positive effect on both flooding and faradaic efficiency, however the stability of the cell was limited. Substitution by another PTFE additive, PTFE NP, was believed to stabilize the cell performance by mitigating the prominence of the cracks.

PTFE NP's were mixed within the catalyst layer showing a positive effect on both the performance and the flooding of the cell.

The largest contribution was attributed to a PTFE dispersion based top layer which was shown to be a key design feature within acidic CO_2R. The stability of this top layer was shown to improve greatly after the use of PTFE NP as a base layer.

The design process resulted in the construction of one of the largest highly acidic (pH<1) cells to date with a faradaic efficiency towards C2+ products of over 50%.

Regarding the continuance of the cell design, the following design steps are believed to enable increased C2+ product formation.

8.1. Cell design

Substrate

As was earlier highlighted within chapter 2, utilizing a PTFE membrane boasts significant advantage compared to carbon paper. Especially in a path towards industrialization a PTFE membrane would be preferred due to its low cost, easy production and both chemical as mechanical robustness. As was proven by [11], the conductivity problem could be omitted by the use of a coated copper current collector. Additionally the results on top layer stability due to the application of PTFE NP instead of PTFE dispersion suggests the use of PTFE membrane. Use of a PTFE membrane might solve the entire stability issue and should therefore most definitely be pursued. An initial design was conceived and is described in the Appendix.

Top layer
The current top layer has been designed purely on the characteristic of hydrophobicity. [76] and [60] both boast a cation stabilizing top layer with even higher C2+ production formation then reported in this thesis. It is recommended to evaluate the working of these top layers.

Catalyst layer impurities
A topic which could not be evaluated but would be of great interest is the application of a bimetallic catalyst. As described in subsection 2.4.3, both the ethanol/ethylene ratio could significantly be improved along with the overall faradaic efficiency towards C2+ products. Highlighted metals are silver and palladium. As a binder it is suggested to substitute Nafion for PVDF to further increase the ethanol of ethylene ration as suggested by [4], PTFE dispersion might be similarly useful.

Electrolyte
Lastly the electrolyte is believed to enable additional productivity towards desired products, the use of Cs is proven to be effective along a wide variety of cell designs, suggesting a similar working on acidic cells. As the electrolyte does not degrade this relatively expensive compound is reduced in costs.
Additionally the use of a stronger acid is believed to increase the local pH at the catalyst surface. subsection 2.4.2 describes the reduced performance associated with increasing buffering capacity. Sulfate is an even stronger acid then phosphate and might thus increase the performance.
Lastly, as indicated within subsection 2.5.3, there is a knowledge gap regarding the benefits or disadvantages of the use of electrolytes prepared with K_2SO_4 and H_2SO_4. These electrolytes have the advantage of a higher pH but have a reduced potassium presence. More research should be done regarding the influence on performance and the stability of these electrolytes.

8.2. Extraction of ethanol
Although included in the appendix, ethanol has been shown to permeate through a Nafion membrane at relevant ethanol concentration of at least 1 wt%. It was observed that no research has been conducted on the transport of ethanol through a Nafion membrane at these concentrations. Preliminary experiments as described in section A.3, show a significant transport at relevant concentrations. This subject should most definitely be researched as the implications on feasibility of ethanol production via the chosen cell design could be severe.

References

[1] R. Tufa et al. “Towards highly efficient electrochemical CO2 reduction: Cell designs, membranes and electrocatalysts”. In: *Applied energy* 277 (2020), p. 115557. DOI: https://doi.org/10.1016/j.apenergy.2020.115557. URL: https://www.sciencedirect.com/science/article/pii/S0306261920310692.

[2] A. J. Bard, G. Inzelt, and F. Scholz. *Electrochemical Dictionary*. 2nd ed. Berlin: Springer Berlin, 2012. DOI: https://doi.org/10.1007/978-3-642-29551-5.

[3] Francesco Bernasconi et al. “Enhancing C ≥2 product selectivity in electrochemical CO 2 reduction by controlling the microstructure of gas diffusion electrodes”. In: *EES Catalysis* 1 (Aug. 2023). DOI: 10.1039/D3EY00140G.

[4] Chaojie Chen et al. “Modulating local environment for electrocatalytic CO2 reduction to alcohol”. In: *Nano Energy* 126 (2024), p. 109656. ISSN: 2211-2855. DOI: https://doi.org/10.1016/j.nanoen.2024.109656. URL: https://www.sciencedirect.com/science/article/pii/S221128552400404X.

[5] Chi Chen, Juliet F. Khosrowabadi Kotyk, and Stafford W. Sheehan. “Progress toward Commercial Application of Electrochemical Carbon Dioxide Reduction”. In: *Chem* 4.11 (2018), pp. 2571–2586. DOI: https://doi.org/10.1016/j.chempr.2018.08.019. URL: https://www.sciencedirect.com/science/article/pii/S2451929418303711.

[6] Chunjun Chen et al. “Highly Efficient Electroreduction of CO2 to C2+ Alcohols on Heterogeneous Dual Active Sites”. In: *Angewandte Chemie International Edition* 59 (June 2020). DOI: 10.1002/anie.202006847.

[7] Cao Thang Dinh et al. “CO 2 electroreduction to ethylene via hydroxide-mediated copper catalysis at an abrupt interface”. In: *Science* 360 (May 2018), pp. 783–787. DOI: 10.1126/science.aas9100.

[8] B. Endrődi et al. “Multilayer Electrolyzer Stack Converts Carbon Dioxide to Gas Products at High Pressure with High Efficiency”. In: *ACS Energy Letters* 4.7 (2019), pp. 1770–1777. DOI: 10.1021/acsenergylett.9b01142. URL: https://doi.org/10.1021/acsenergylett.9b01142.

[9] Balázs Endrődi et al. “High carbonate ion conductance of a robust PiperION membrane allows industrial current density and conversion in a zero-gap carbon dioxide electrolyzer cell”. In: *Energy and Environmental Science* 13 (Sept. 2020). DOI: 10.1039/D0EE02589E.

[10] Björn Eriksson et al. “Mitigation of Carbon Crossover in CO2 Electrolysis by Use of Bipolar Membranes”. In: *Journal of The Electrochemical Society* 169 (Mar. 2022). DOI: 10.1149/1945-7111/ac580e.

[11] Michael Filippi et al. “Scale-Up of PTFE-Based Gas Diffusion Electrodes Using an Electrolyte-Integrated Polymer-Coated Current Collector Approach”. In: *ACS Energy Letters* 9 (Mar. 2024), pp. 1361–1368. DOI: 10.1021/acsenergylett.4c00114.

[12] Michael Filippi et al. “Understanding the Impact of Catholyte Flow Compartment Design on the Efficiency of CO2 Electrolyzers”. In: *Energy and Environmental Science* 16 (Jan. 2023). DOI: 10.1039/D3EE02243A.

[13] Christine M. Gabardo et al. “Continuous Carbon Dioxide Electroreduction to Concentrated Multicarbon Products Using a Membrane Electrode Assembly”. In: *Joule* 3.11 (2019), pp. 2777–2791. ISSN: 2542-4351. DOI: https://doi.org/10.1016/j.joule.2019.07.021. URL: https://www.sciencedirect.com/science/article/pii/S2542435119303654.

[14] Alina Gawel et al. “Electrochemical CO2 reduction - The macroscopic world of electrode design, reactor concepts and economic aspects”. In: *iScience* 25.4 (2022), p. 104011. ISSN: 2589-0042. DOI: https://doi.org/10.1016/j.isci.2022.104011. URL: https://www.sciencedirect.com/science/article/pii/S2589004222002814.

[15] Jeffery B. Greenblatt et al. “The Technical and Energetic Challenges of Separating (Photo)Electrochemical Carbon Dioxide Reduction Products”. In: *Joule* 2.3 (2018), pp. 381–420. ISSN: 2542-4351. DOI: https://doi.org/10.1016/j.joule.2018.01.014. URL: https://www.sciencedirect.com/science/article/pii/S2542435118300424.

[16] R. Gary Grim et al. “Transforming the carbon economy: challenges and opportunities in the convergence of low-cost electricity and reductive CO2 utilization”. In: *Energy Environ. Sci.* 13 (2 2020), pp. 472–494. DOI: 10.1039/C9EE02410G. URL: http://dx.doi.org/10.1039/C9EE02410G.

[17] Zhengxiang Gu et al. “Efficient Electrocatalytic CO2 Reduction to C2+ Alcohols at Defect-Site-Rich Cu Surface”. In: *Joule* 5 (Jan. 2021). DOI: 10.1016/j.joule.2020.12.011.

[18] Hilmar Guzmán, Nunzio Russo, and Simelys Hernández. “CO2 valorisation towards alcohols by Cu-based electrocatalysts: challenges and perspectives”. In: *Green Chem.* 23 (5 2021), pp. 1896–1920. DOI: 10.1039/D0GC03334K. URL: http://dx.doi.org/10.1039/D0GC03334K.

[19] N. Habbache et al. “Leaching of copper oxide with different acid solutions”. In: *Chemical Engineering Journal* 152.2 (2009), pp. 503–508. ISSN: 1385-8947. DOI: https://doi.org/10.1016/j.cej.2009.05.020. URL: https://www.sciencedirect.com/science/article/pii/S1385894709003921.

[20] Hyunsu Han et al. “Selective Electrochemical CO 2 Conversions to Multicarbon Alcohols on Highly Efficient N-doped Porous Carbon-supported Cu Catalysts”. In: *Green Chemistry* 22 (Oct. 2019). DOI: 10.1039/C9GC03088C.

[21] Rudolf Holze. “Buchbesprechung: Electrochemical Methods. Fundamentals and Applications. Von Allen J. Bard und Larry R. Faulkner”. In: *Angewandte Chemie* 114 (Feb. 2002), pp. 677–680. DOI: 10.1002/1521-3757(20020215)114:43.0.CO;2-N.

[22] Y. Hori. *Electrochemical CO2 Reduction on Metal Electrodes-Modern Aspects of Electrochemistry*. Ed. by Constantinos G. Vayenas, Ralph E. White, and Maria E. Gamboa-Aldeco. New York: Springer New York, 2008, pp. 157–161. DOI: 10.1007/978-0-387-49489-0_3. URL: https://doi.org/10.1007/978-0-387-49489-0_3.

[23] Jianan Erick Huang et al. “CO₂ electrolysis to multicarbon products in strong acid”. In: *Science* 372.6546 (2021), pp. 1074–1078. DOI: 10.1126/science.abg6582. URL: https://www.science.org/doi/abs/10.1126/science.abg6582.

[24] Jianan Erick Huang et al. “CO2 electroreduction to multicarbon products in strongly acidic electrolyte via synergistically modulating the local microenvironment”. In: *Nature communications* 13.7596 (2022). DOI: https://doi-org.tudelft.idm.oclc.org/10.1038/s41467-022-35415-x. URL: https://doi.org/10.1038/s41467-022-35415-x.

[25] Wei-Dong Huang and Y.-H. Percival Zhang. “Analysis of biofuels production from sugar based on three criteria: Thermodynamics, bioenergetics, and product separation”. In: *Energy Environ. Sci.* 4 (3 2011), pp. 784–792. DOI: 10.1039/C0EE00069H. URL: http://dx.doi.org/10.1039/C0EE00069H.

[26] Faria Huq et al. “Influence of the PTFE Membrane Thickness on the CO 2 Electroreduction Performance of Sputtered Cu□PTFE Gas Diffusion Electrodes”. In: *ChemElectroChem* 9 (Jan. 2022). DOI: 10.1002/celc.202101279.

[27] Hugo-Pieter Iglesias van Montfort et al. “Non-invasive current collectors for improved current-density distribution during CO 2 electrolysis on super-hydrophobic electrodes”. In: (May 2023). DOI: 10.21203/rs.3.rs-2938282/v1.

[28] M Ise, K.D Kreuer, and J Maier. “Electroosmotic drag in polymer electrolyte membranes: an electrophoretic NMR study”. In: *Solid State Ionics* 125.1 (1999), pp. 213–223. ISSN: 0167-2738. DOI: https://doi.org/10.1016/S0167-2738(99)00178-2. URL: https://www.sciencedirect.com/science/article/pii/S0167273899001782.

[29] Masao Iwai, Hiroshi Majima, and Yasuhiro Awakura. “Dissolution of copper in hydrochloric acid solutions with dissolved molecular oxygen”. In: *Hydrometallurgy* 20.1 (1988), pp. 87–95. ISSN: 0304-386X. DOI: https://doi.org/10.1016/0304-386X(88)90028-X. URL: https://www.sciencedirect.com/science/article/pii/0304386X8890028X.

[30] Theresa Jaster et al. “Electrochemical CO2 reduction toward multicarbon alcohols - The microscopic world of catalysts and process conditions”. In: *iScience* 25.4 (2022), p. 104010. ISSN: 2589-0042. DOI: https://doi.org/10.1016/j.isci.2022.104010. URL: https://www.sciencedirect.com/science/article/pii/S2589004222002802.

[31] Emily Jeng and Feng Jiao. “Investigation of CO 2 Single-Pass Conversion in a Flow Electrolyzer”. In: *Reaction Chemistry and Engineering* 5 (July 2020). DOI: 10.1039/D0RE00261E.

[32] Yali Ji et al. “Selective CO-to-acetate electroproduction via intermediate adsorption tuning on ordered Cu-Pd sites”. In: *Nature Catalysis* 5 (4 Nov. 2020). DOI: 10.21203/rs.3.rs-111772/v1.

[33] Md Kibria et al. “Electrochemical CO 2 Reduction into Chemical Feedstocks: From Mechanistic Electrocatalysis Models to System Design”. In: *Advanced Materials* 31 (May 2019), p. 1807166. DOI: 10.1002/adma.201807166.

[34] Byoungsu Kim et al. “Effects of composition of the micro porous layer and the substrate on performance in the electrochemical reduction of CO2 to CO”. In: *Journal of Power Sources* 312 (2016), pp. 192–198. ISSN: 0378-7753. DOI: https://doi.org/10.1016/j.jpowsour.2016.02.043. URL: https://www.sciencedirect.com/science/article/pii/S0378775316301501.

[35] E. W. Lees et al. “Gas diffusion electrodes and membranes for CO2 reduction electrolysers”. In: *Nature Reviews Materials* 7 (2022), pp. 55–64. DOI: 10.1038/s41578-021-00356-2. URL: https://doi.org/10.1038/s41578-021-00356-2.

[36] Fengwang Li et al. “Cooperative CO2-to-ethanol conversion via enriched intermediates at molecule–metal catalyst interfaces”. In: *Nature Catalysis* 3 (Jan. 2020), pp. 1–8. DOI: 10.1038/s41929-019-0383-7.

[37] Hongqing Liang et al. “Hydrophobic Copper Interfaces Boost Electroreduction of Carbon Dioxide to Ethylene in Water”. In: *ACS Catalysis* 11 (Jan. 2021), pp. 958–966. DOI: 10.1021/acscatal.0c03766.

[38] Shuyu Liang et al. “Electrolytic cell design for electrochemical CO2 reduction”. In: *Journal of CO2 Utilization* 35 (2020), pp. 90–105. DOI: https://doi.org/10.1016/j.jcou.2019.09.007. URL: https://www.sciencedirect.com/science/article/pii/S2212982019308261.

[39] Yanrong Liu et al. “Recent progress on electrochemical reduction of CO2 to methanol”. In: *Current Opinion in Green and Sustainable Chemistry* 23 (2020), pp. 10–17. ISSN: 2452-2236. DOI: https://doi.org/10.1016/j.cogsc.2020.03.009. URL: https://www.sciencedirect.com/science/article/pii/S2452223620300262.

[40] Jing-Jing Lv et al. “A Highly Porous Copper Electrocatalyst for Carbon Dioxide Reduction”. In: *Advanced Materials* 30 (Oct. 2018). DOI: 10.1002/adma.201803111.

[41] Wenchao Ma et al. “Electrocatalytic reduction of CO2 to ethylene and ethanol through hydrogen-assisted C–C coupling over fluorine-modified copper”. In: *Nature Catalysis* 3 (June 2020), pp. 1–10. DOI: 10.1038/s41929-020-0450-0.

[42] Christopher McCallum et al. “Reducing the crossover of carbonate and liquid products during carbon dioxide electroreduction”. In: *Cell Reports Physical Science* 2.8 (2021), p. 100522. ISSN: 2666-3864. DOI: https://doi.org/10.1016/j.xcrp.2021.100522. URL: https://www.sciencedirect.com/science/article/pii/S2666386421002265.

[43] Rui Kai Miao et al. “Electroosmotic flow steers neutral products and enables concentrated ethanol electroproduction from CO2”. In: *Joule* 5.10 (2021), pp. 2742–2753. ISSN: 2542-4351. DOI: https://doi.org/10.1016/j.joule.2021.08.013. URL: https://www.sciencedirect.com/science/article/pii/S2542435121003974.

[44] Endre Nagy et al. “Analysis of energy saving by combination of distillation and pervaporation for biofuel production”. In: *Chemical Engineering and Processing: Process Intensification* 98 (2015), pp. 86–94. ISSN: 0255-2701. DOI: https://doi.org/10.1016/j.cep.2015.10.010. URL: https://www.sciencedirect.com/science/article/pii/S0255270115301215.

[45] Stephanie Nitopi et al. “Progress and Perspectives of Electrochemical CO2 Reduction on Copper in Aqueous Electrolyte”. In: *Chemical Reviews* 119.12 (2019), pp. 7610–7672. DOI: 10.1021/acs.chemrev.8b00705. URL: https://doi.org/10.1021/acs.chemrev.8b00705.

[46] Adnan Ozden et al. “Cascade CO2 electroreduction enables efficient carbonate-free production of ethylene”. In: *Joule* 5.3 (2021), pp. 706–719. ISSN: 2542-4351. DOI: https://doi.org/10.1016/j.joule.2021.01.007. URL: https://www.sciencedirect.com/science/article/pii/S2542435121000386.

[47] Adnan Ozden et al. “High-Rate and Efficient Ethylene Electrosynthesis Using a Catalyst/Promoter/Transport Layer”. In: *ACS Energy Letters* 5.9 (2020), pp. 2811–2818. DOI: 10.1021/acsenergylett.0c01266. URL: https://doi.org/10.1021/acsenergylett.0c01266.

[48] Ilhwan Park et al. “Leaching of Copper from Cuprous Oxide in Aerated Sulfuric Acid”. In: *MATERIALS TRANSACTIONS* 58 (Aug. 2017). DOI: 10.2320/matertrans.M2017147.

[49] Mahinder Ramdin et al. “Carbonation in Low-Temperature CO2 Electrolyzers: Causes, Consequences, and Solutions”. In: *Industrial and Engineering Chemistry Research* 62.18 (2023), pp. 6843–6864. DOI: 10.1021/acs.iecr.3c00118. URL: https://doi.org/10.1021/acs.iecr.3c00118.

[50] Mahinder Ramdin et al. “Electroreduction of CO2/CO to C2 Products: Process Modeling, Downstream Separation, System Integration, and Economic Analysis”. In: *Industrial and Engineering Chemistry Research* 60.49 (Nov. 2021), pp. 17862–17880. ISSN: 1520-5045. DOI: 10.1021/acs.iecr.1c03592. URL: http://dx.doi.org/10.1021/acs.iecr.1c03592.

[51] Dan Ren et al. “Atomic Layer Deposition of ZnO on CuO Enables Selective and Efficient Electroreduction of Carbon Dioxide to Liquid Fuels”. In: *Angewandte Chemie (International ed. in English)* 58 (Aug. 2019). DOI: 10.1002/anie.201909610.

[52] Joaquin Resasco et al. “Effects of Anion Identity and Concentration on Electrochemical Reduction of CO2”. In: *ChemElectroChem* 5 (Jan. 2018). DOI: 10.1002/celc.201701316.

[53] S. R. Samms, S. Wasmus, and R. F. Savinell. “Thermal Stability of Nafion® in Simulated Fuel Cell Environments”. In: *Journal of The Electrochemical Society* 143.5 (May 1996), p. 1498. DOI: 10.1149/1.1836669. URL: https://dx.doi.org/10.1149/1.1836669.

[54] S.M. Mayanna. T.H.V. Setty. “Role of chloride ions in relation to copper corrosion and inhibition”. In: *Proceedings of the Indian Academy of Sciences - Section A* 80.4 (1974), pp. 184–193. ISSN: 0370-0089. DOI: 10.1007/BF03046676. URL: https://doi.org/10.1007/BF03046676.

[55] D.D. Macdonald. S. Shwarifi-Asl. “Is Copper Immune to Corrosion When in Contact With Water and Aqueous Solutions?” In: (2011). ISSN: 2000-0456. URL: https://www.stralsakerhetsmyndigheten.se/contentassets/d23a452aa5db46b196c729f0c94375db/201109-is-copper-immune-to-corrosion-when-in-contact-with-water-and-aqueous-solutions#:~:text=Thermodynamically%2C%20immunity%20of%20copper%20in,presence%20of%20pure%20anoxic%20water..

[56] C.M. Simon and W. Kaminsky. “Chemical recycling of polytetrafluoroethylene by pyrolysis”. In: *Polymer Degradation and Stability* 62.1 (1998), pp. 1–7. ISSN: 0141-3910. DOI: https://doi.org/10.1016/S0141-3910(97)00097-9. URL: https://www.sciencedirect.com/science/article/pii/S0141391097000979.

[57] Ana Sofia Varela et al. “Controlling the selectivity of CO2 electroreduction on copper: The effect of the electrolyte concentration and the importance of the local pH”. In: *Catalysis Today* 260 (2016). Surface Analysis and Dynamics (SAND), pp. 8–13. ISSN: 0920-5861. DOI: https://doi.org/10.1016/j.cattod.2015.06.009. URL: https://www.sciencedirect.com/science/article/pii/S0920586115003594.

[58] Adam Vass et al. “Anode Catalysts in CO 2 Electrolysis: Challenges and Untapped Opportunities”. In: *ACS Catalysis* 12 (Jan. 2022), pp. 1037–1051. DOI: 10.1021/acscatal.1c04978.

[59] Sumit Verma et al. “Insights into the Low Overpotential Electroreduction of CO2 to CO on a Supported Gold Catalyst in an Alkaline Flow Electrolyzer”. In: *ACS Energy Letters* 3.1 (2018), pp. 193–198. DOI: 10.1021/acsenergylett.7b01096. URL: https://doi.org/10.1021/acsenergylett.7b01096.

[60] Elli Vichou et al. “Tuning Selectivity of Acidic Carbon Dioxide Electrolysis via Surface Modification”. In: *Chemistry of Materials* 35 (Aug. 2023). DOI: 10.1021/acs.chemmater.3c01326.

[61] D. Wakerley, S. Lamaison, and J. Wicks et al. “Gas diffusion electrodes, reactor designs and key metrics of low-temperature CO2 electrolysers”. In: *Nature. energy* 7 (2022), pp. 130–143. DOI: https://doi-org.tudelft.idm.oclc.org/10.1038/s41560-021-00973-9. URL: https://doi.org/10.1021/acsenergylett.7b01017.

[62] Haoyuan Wang et al. “CO2 electrolysis toward acetate: A review”. In: *Current Opinion in Electrochemistry* 39 (2023), p. 101253. ISSN: 2451-9103. DOI: https://doi.org/10.1016/j.coelec.2023.101253. URL: https://www.sciencedirect.com/science/article/pii/S2451910323000467.

[63] Pengtang Wang et al. “Boosting electrocatalytic CO2–to–ethanol production via asymmetric C–C coupling”. In: *Nature Communications* 13 (June 2022), p. 3754. DOI: 10.1038/s41467-022-31427-9.

[64] Shanwen Wang et al. “Electrochemical Reduction of CO2 to Alcohols: Current Understanding, Progress, and Challenges”. In: *Advanced Energy and Sustainability Research* 3 (Sept. 2021). DOI: 10.1002/aesr.202100131.

[65] Tian Wang et al. “The origins of catalytic selectivity for the electrochemical conversion of carbon dioxide to methanol”. In: *Nano Research* (2023). DOI: 10.1007/s12274-023-5653-7. URL: https://www.sciopen.com/article/10.1007/s12274-023-5653-7.

[66] Xue Wang et al. “Efficient electrically powered CO2-to-ethanol via suppression of deoxygenation”. In: *Nature Energy* 5 (June 2020), pp. 1–9. DOI: 10.1038/s41560-020-0607-8.

[67] Yulin Wang et al. “Electro-osmotic drag coefficient of Nafion membrane with low water Content for Proton exchange membrane fuel cells”. In: *Energy Reports* 8 (2022). Selected papers from 2022 7th International Conference on Advances on Clean Energy Research, pp. 598–612. ISSN: 2352-4847. DOI: https://doi.org/10.1016/j.egyr.2022.10.233. URL: https://www.sciencedirect.com/science/article/pii/S2352484722021692.

[68] Kunlanan Wiranarongkorn et al. “A comprehensive review of electrochemical reduction of CO2 to methanol: Technical and design aspects”. In: *Journal of CO2 Utilization* 71 (2023), p. 102477. ISSN: 2212-9820. DOI: https://doi.org/10.1016/j.jcou.2023.102477. URL: https://www.sciencedirect.com/science/article/pii/S2212982023000884.

[69] Yuming Wu et al. “Mitigating Electrolyte Flooding for Electrochemical CO 2 Reduction via Infiltration of Hydrophobic Particles in a Gas Diffusion Layer”. In: *ACS Energy Letters* 7 (Aug. 2022), pp. 2884–2892. DOI: 10.1021/acsenergylett.2c01555.

[70] Yi Xie et al. “High carbon utilization in CO2 reduction to multi-carbon products in acidic media”. In: *Nature Catalysis* 5 (June 2022), pp. 1–7. DOI: 10.1038/s41929-022-00788-1.

[71] Zhuo Xing et al. “Enhancing carbon dioxide gas-diffusion electrolysis by creating a hydrophobic catalyst microenvironment”. In: *Nature Communications* 12 (Jan. 2021). DOI: 10.1038/s41467-020-20397-5.

[72] Yi Xu et al. “Self-Cleaning CO2 Reduction Systems: Unsteady Electrochemical Forcing Enables Stability”. In: *ACS Energy Letters* 6.2 (2021), pp. 809–815. DOI: 10.1021/acsenergylett.0c02401. URL: https://doi.org/10.1021/acsenergylett.0c02401.

[73] Kailun Yang et al. “Role of the Carbon-Based Gas Diffusion Layer on Flooding in a Gas Diffusion Electrode Cell for Electrochemical CO2 Reduction”. English. In: *ACS Energy Letters* 6.1 (2021), pp. 33–40. ISSN: 2380-8195. DOI: 10.1021/acsenergylett.0c02184.

[74] Zhe Yao and Rui Lin. “Overcoming Low C 2+ Yield in Acidic CO 2 Electroreduction: Modulating Local Hydrophobicity for Enhanced Performance”. In: *Small* (Dec. 2023). DOI: 10.1002/smll.202306686.

[75] Jiawei Zhang et al. “Steering CO2 electroreduction pathway toward ethanol via surface-bounded hydroxyl species-induced noncovalent interaction”. In: *Proceedings of the National Academy of Sciences of the United States of America* 120 (Mar. 2023), e2218987120. DOI: 10.1073/pnas.2218987120.

[76] Yong Zhao et al. “Conversion of CO_2 to multicarbon products in strong acid by controlling the catalyst microenvironment”. In: *Nature Synthesis* 2.5 (May 2023), pp. 403–412. DOI: 10.1038/s44160-022-00234-x. URL: https://ui.adsabs.harvard.edu/abs/2023NatSy...2..403Z.

[77] T-T Zhuang et al. “Steering post-C–C coupling selectivity enables high efficiency electroreduction of carbon dioxide to multi-carbon alcohols”. In: *Nature Catalysis* 1 (June 2018). DOI: 10.1038/s41929-018-0084-7.

A

A.1. PTFE-membrane cell design

A.1.1. Current collector

The current collectors utilized within this report have been based upon the designs by [11]. This article outlines one of the first successful approaches on scaled-up PTFE membrane based design and has proven its performance on 100 cm^2. The electrons are provided via the front via a copper current collector pressed against the catalyst layer. Two designs have been created and are depicted in Figure A.1a and Figure A.1b, the red squares visualize the uncoated area. The first design is a simple grid, boosting a relatively short distances to the catalyst layer compared to the second design. A disadvantage about this grid is how it is expected to disturb the flow significantly and thereby disturb the alkaline electrolyte layer vital for C-product formation. The second design aims to reduce this issue and is inspired on the flow field as modelled via CFD [12] although the validity of the CFD model is questionable both due to the relatively large presence of hydrogen formation on the catalyst layer and addition of a current collector. Both current collectors have been coated with PEEK with a thickness of 25-60µm to prevent activity of the collector and have been designed to support a comparable active catalyst area of 368.64 and 369.15 mm^2. Furthermore the maximum distance between catalyst and current collector are comparable with 2,4 mm for the grid and ±2.1 mm for the leaf design respectively. Differences include the average distance between a point on the catalyst layer and the nearest arm of the current collector, this is believed to manifest itself via an increased voltage required for similar current densities.

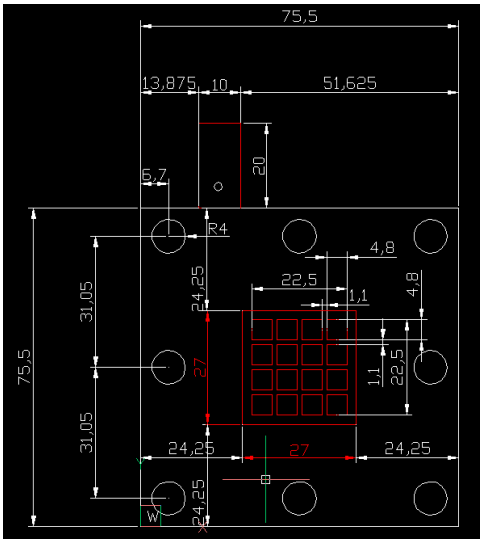

(a) Grid Current collector

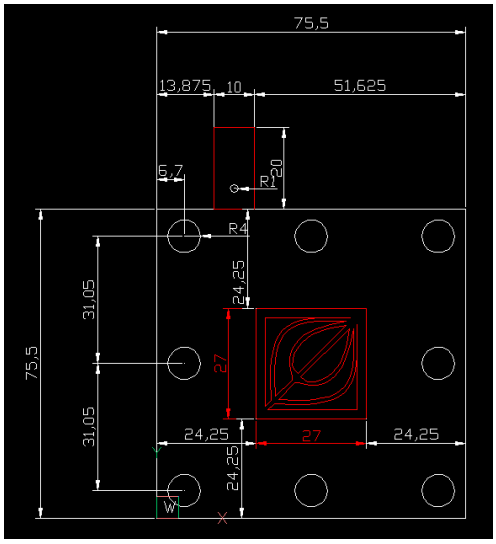

(b) Leaf Current Collector design

Figure A.1

The current collectors were coated by the Company Rhenotherm which offered quick and cheap coating with the additional advantage of masking the conductive areas to enable omission of the described engraving step in [11]. Unfortunately the technique used by the company was proven insufficient to coat the surfaces within the grid, leaving a large surface of exposed copper. It is recommended for further steps to use the Company ACS Coating Systems which have proven their ability, and subsequent engraving to remove coating from conductive areas.

Alternatives like copper tape and a copper plate with kapton tape showed to be impractical causing CO2 leakage, electrolyte leakage or in the case of kapton tape unwanted reactions via exposed glue. The design described above has been tested on all of these things and could be readily integrated in the cell architecture used if properly coated.

A.2. Additional tables and figures

$2H^+ + 2e^- \rightarrow H_{2\,(g)}$	E^0 (V vs. RHE) = 0 V	(1)
$CO_2 + 2H^+ + 2e^- \rightarrow CO_{\,(g)} + H_2O$	E^0 (V vs. RHE) = −0.10 V	(2)
$CO_2 + 6H^+ + 6e^- \rightarrow CH_3OH_{\,(l)} + H_2O$	E^0 (V vs. RHE) = 0.03 V	(3)
$CO_2 + 2H^+ + 2e^- \rightarrow HCOOH_{\,(l)}$	E^0 (V vs. RHE) = −0.12 V	(4)
$CO_2 + 8H^+ + 8e^- \rightarrow CH_{4\,(g)} + 2H_2O$	E^0 (V vs. RHE) = 0.17 V	(5)
$2CO_2 + 12H^+ + 12e^- \rightarrow C_2H_{4\,(g)} + 4H_2O$	E^0 (V vs. RHE) = 0.08 V	(6)
$2CO_2 + 12H^+ + 12e^- \rightarrow C_2H_5OH_{\,(l)} + 3H_2O$	E^0 (V vs. RHE) = 0.09 V	(7)
$2CO_2 + 10H^+ + 10e^- \rightarrow CH_3CHO_{\,(l)} + 3H_2O$	E^0 (V vs. RHE) = 0.06 V	(8)
$2CO_2 + 8H^+ + 8e^- \rightarrow CH_3COOH_{\,(l)} + 2H_2O$	E^0 (V vs. RHE) = 0.11 V	(9)
$3CO_2 + 18H^+ + 18e^- \rightarrow C_3H_7OH_{\,(l)} + 5H_2O$	E^0 (V vs. RHE) = 0.10 V	(10)
$4OH^- \rightarrow O_{2\,(g)} + 2H_2O + 4e^-$	E^0 (V vs. RHE) = 1.23 V	(11)

Figure A.2: Relevant half-reactions within CO_2R.

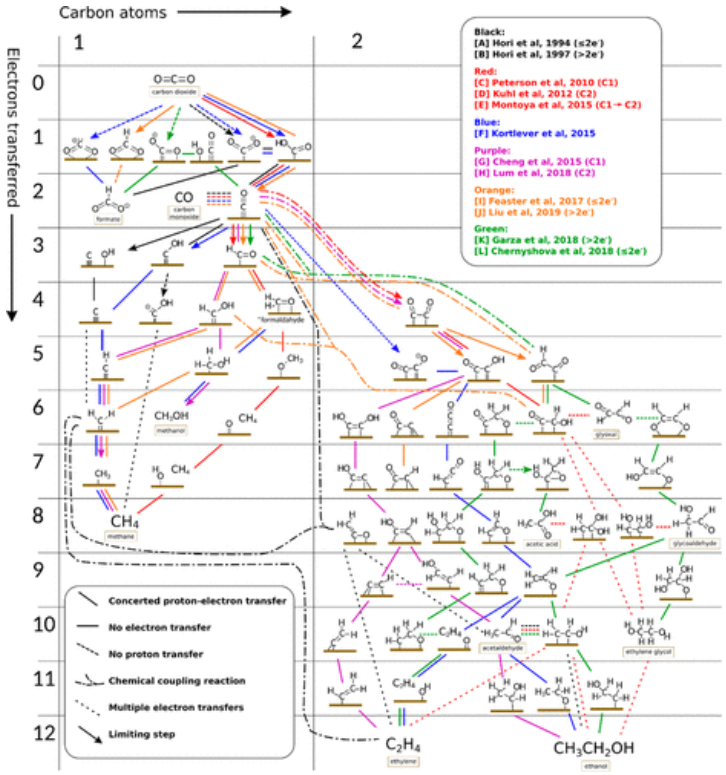

Figure A.3: Graphical depiction of reaction pathways towards products, note the resemblance between ethylene and ethanol.

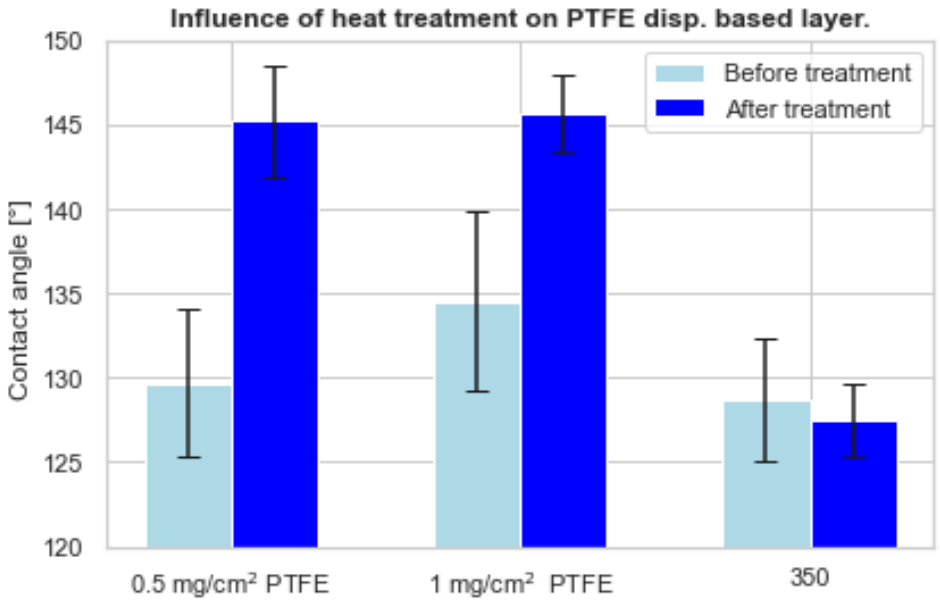

Figure A.4: Influence of heat treatment at 250°C for 2 hours on the hydrophobicity of a PTFE disp. based layer, additionally with in the last column severe degradion at 350 °C was demonstrated

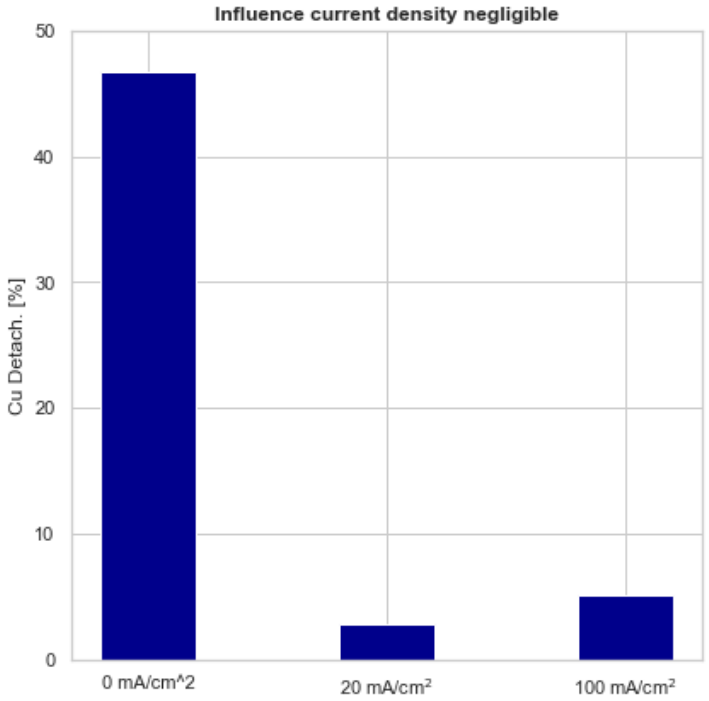

Figure A.5: The current density applied had no significant effect on the deterioration of the catalyst layer

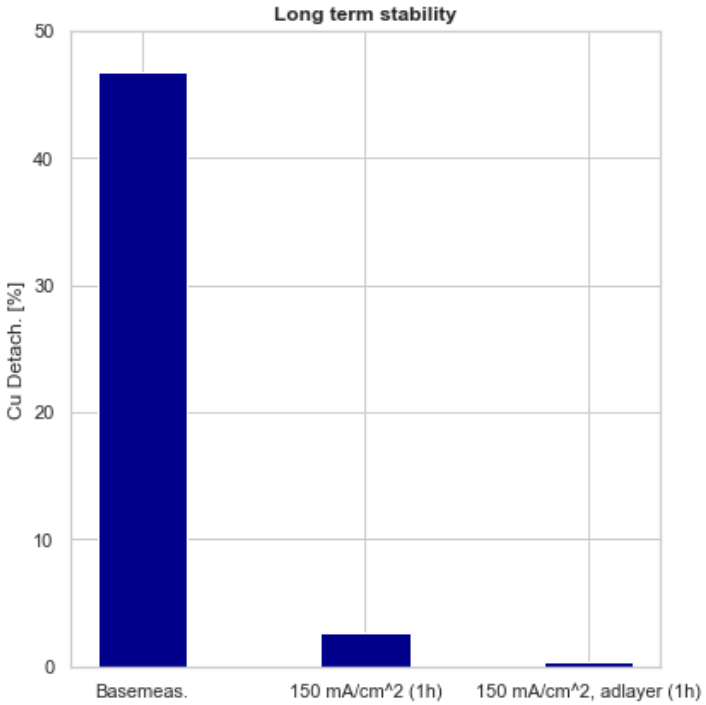

Figure A.6: Confirmation of long term stability of the catalyst layer. With on the left the baseline measurement, in the middle a regular Cu coated carbon GDL and on the right PTFE NP-Cu/PTFE-PTFE type GDE.

	Catholyte		**Anolyte**	
	pH	Cond. [mS/cm]	pH	Cond. [mS/cm]
Initial	0.96	260.5	0.90	57.3
150 mA/cm	0.96	250.6	0.83	75.08
250 mA/cm	1.00	244.3	0.81	66.95
350 mA/cm	1.04	239,6	0.87	54.84

Table A.1: Table describing the pH and conductivity of the described catholyte and anolyte after 1 hour of operation concerning the tests in subsection 6.3.3

Interestingly the pH of the anolyte acidified while the catholyte increased in pH. This phenomenon can be explained by the osmotic pressure of dissolved KCl in the catholyte. A similar path considering the pH was observed in literature [23].

Conf.	Catalyst	Remarks	Catholyte	Stab. [h]	J [mA/cm^2]	V	FE [%]					Source
							H_2	$C2^+$	EtOH	PrOH	Alc./C_2H_4	
4AxN	Defect site rich Cu,	CuCl elec reduced Then spraycoated	None	30	200	3.5	19	66	45	15	10.9	[17]
4AxN	FeTPP[Cl]/Cu(111)		None	15	580	3.7	5	82	40	3	1.1	[36]
2AHH	NGQ/Cu_nr(111)	63% Pyri. N	1 M KOH	100	282	0.9*	10	82	45	8	2.2	[6]
2AHH	Elec. red. CuO	Reduced on cathode	1 M KOH	2	200	0.6*	13	47	10	7	0.6	[40]
4AxN	Cu_2O(200)/Ag(111)	Cu reduced on cathode, 2.3wt% Ag	None	12	800	4.79	8	80	39	3	1.2	[63]
2AHH			1 M KOH	6	800	0.89*	10	78	38	3	1.1	
4AxN	34%N-C/Cu	62% Pyri N	None	15	160	3.67	4	95	52	2	1.4	[66]
2AHH	ZnCu	ZnO sputtered on CuO Elec. reduced on cathode	1M KOH	10	200	0.68*	20	67	41	6	2.6	[51]
2AHH	Cu_2S-Cu NP	Vacancy enriched Cu shell Around Cu2S NP	1 M KOH	2.5	400	0.92*	13	59	25	7	1.5	[77]
3AHH	Elec. red. CuO(110)	Reduced on cathode	3 M KOH	7	1000	0.87*	8	91	40	6	1.1	[75]
2CLL	Cu sputtered Cu/C NP mix	K+ active PFSA layer Carbon layer	1 M H_3PO_4 3 M KCl	12	1200	4.2	42	40	11	4	0,7	[23]
3CLL	Elec. red. CuO	Reduced on cathode	0.05 H_2SO_4 3 M KCl	30	700	1.48*	5	79	23	10	0.7	[24]
2CLL	Cu sputtered	K+ active PFSA layer COF layer for PFSA orient.	1 M H_3PO_4 3 M KCl	30	200	2.4**	10	75	26	0	0.6	[76]
2CLL	Cu NP	Custom Hydroph. GDE PTFE/C based ink	0.5 M K_2SO_4 x H_2SO_4 (pH=2)	50	300	1.2*	17	62	-	-	-	[74]
3CLL	Cu Pd(6.2%)	Cu sputtered on PTFE Galvanic repl. by $PdCl_2$	0.5 M K_2SO_4 x H_2SO_4 (pH=2)	4.5	500	1*	9.1	87.1	34.5	3.2	0.83	[70]

Table A.2: State of the art EtOH aimed cells above 100 mA/cm^2 with a stability of at least 2 hour, *shows cathodic voltage vs RHE, **shows cathodic voltage vs Ag/AgCl

A.3. Preliminary ethanol diffusion tests

A multitude of techno-economic analyses utilize a concentration of 10wt% of ethanol within their calculations [50] [33]. However, as stated before, a large gap of knowledge was observed as to the feasibility of these high concentrations in CO2 reduction systems utilizing a CEM membrane. Within this section an initial attempt has been made to reduce this gap and examine the potential of Nafion membranes for creation of high concentration liquid products.

A.3.1. Test Set-up

The diffusion of ethanol through a Nafion 117 membrane with a thickness of ±180 microns was measured in the general cell set-up described in the test set-up section with the following exceptions.

1. The cathodic gas inlet and outlet tubes were sealed, no CO2 was supplied to the system.
2. A blank carbon GDE was used as to create only hydrogen under potential.
3. 50 ml of 1 molar H_3PO_4 electrolyte with a to be described molarity of ethanol was supplied to the cathode, 50 ml of 1 molar H_3PO_4 solution was used as anolyte.

Samples were taken regularly throughout the duration of the test via a an airtight T-valve using a pipette with a volume of around 0.2 ml, for each sample a first sample of 0.25 ml was taken and thrown out to ensure fresh catholyte in the second sample. A total of 7.5 ml of electrolyte was taken during the duration of each test. Both the catholyte and the anolyte were open to air via 1 tube, additionally to measure the evaporation of ethanol via the gaseous outlet tube, the gaseous outlet tube of the catholyte was led through an icebath. In case of an applied potential, chronopotentiometry was applied to ensure a constant current density of 200 mA/cm^2 yielding a total current of 1 A. Two concentrations were tested of 0.25 M EtOH and 0.75 M EtOH, corresponding to approximately 1 and 3 wt% respectively. A fresh Nafion membrane was used for each experiment.

A.3.2. Experiments

In order to assess the influence of a potential electro-osmotic drag coefficient as described in [21], two tests were executed with each mixture, one without potential and one with a potential. Both the cathodic and the anodic concentrations were monitored over a period of 3 hour and are displayed in Figure A.7.

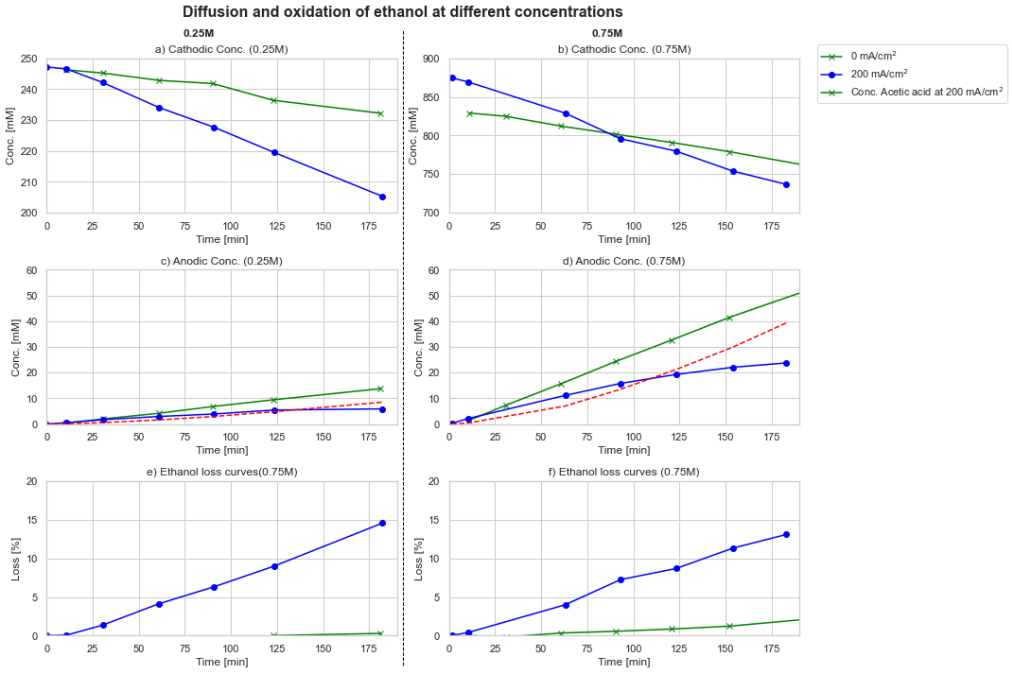

Figure A.7: a,b) Cathodic concentrations of ethanol over time, **c,d)** Anodic concentrations over time of both EtOH and acetic acid in the case of chronopotentiometric tests, **e,f)** Total ethanol loss within the system.

As is to be read from the figure a clear pattern is revealed, for both concentrations tested application of a potential induces a fastened decline of the cathodic ethanol concenctration. Additionally, looking at figures c and d, the anodic concentration increases more rapidly if no current is present suggesting a high rate of oxidation, further demonstrated by the high concentrations of acetic acid, one of the oxidation products of ethanol The last curves (e,f) show the loss of ethanol within the system, showing little to no loss of ethanol is observed without a potential. As will be described subsection A.3.3 the concentrations measured might provide a skewered image due to the electro-osmotic drag induced water transport from anode to cathode.

Ethanol reduction on the cathode has been ruled out as no new products have been observed via the HPLC measurements except for minor quantities of acetic acid (<5 mM) which diffused from the anode towards the cathode.

As no distinction can be made between the influence of an electro-osmotic drag coefficient and diffusion, a combined coefficient is calculated hereafter called ”Transport coefficient”. The transport coefficient has been calculated via a numerical model, the model linearizes the anodic concentration and subsequently determines a numerical estimation of the transport coefficient via minimization of normalized RMSE. A fitting of the anodic concentration instead of a numerical approximation as to exclude oxidation of ethanol as a factor. The transport coefficient is calculated and summarized in Table A.3. Note that these transport coefficients include a potential electro-osmotic drag coefficient.

	0.25 M	**0.75 M**	**Ratio**
No pot.	9,86E-8	1.32E-7	1,34
Pot.	2,93E-7	2.87E-7	0,98

Table A.3: Calculated migration coefficients

A clear difference in combined transport coefficient is observed as the average with a potential is over 2.5 times as great as without. As a potential electro-osmotic drag coefficient on ethanol should act in the direction of the protonflux this is an unexpected result. However, taking into account the possible electro-osmotic drag coefficient on water and its associated migration inducing up to 20% error after three hours regarding the measurements as discussed in subsection A.3.3, the actual transport coefficient of ethanol with a potential on might actually be lower.

As modelling of the ethanol concentrations through the use of a oxidation coefficient was deemed to be unsatisfactory, a test with a duration of 7 hours was done to enable an estimation on the equilibrium conditions if a wt% of 3 would be sustained at the catholyte side. A current density of 200 mA/cm^2 was applied throughout the entire period. After three hours of circulating catholyte the set-up was altered via a set of tubes to provide a catholyte stream with constant properties, this stream was not recirculated and only passed the cathode once. On the anode side, no change in anolyte was made.

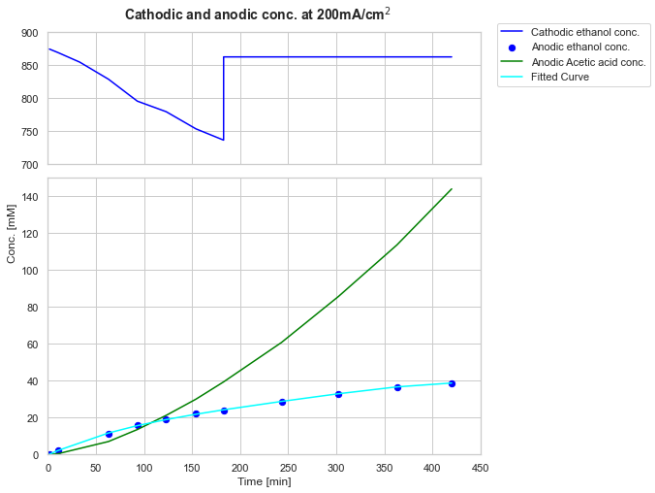

Figure A.8: Long duration ethanol transport test at 200 mA/cm^2 on a bare carbon GDL. With the upper figure describing the cathodic ethanol concentration and the lower figure describing the anodic ethanol and acetic acid concentration. A stream of constant ethanol concentration was used after three hours.

Interestingly the concentration of acetic acid far exceed the anodic concentration of ethanol, as acetic acid is an oxidation product of ethanol this gives an additional insight on the quantity of ethanol that has crossed the membrane and on the severity of oxidation of ethanol.

The results considering the anodic ethanol concentration were fitted with a polynomial curve and estimated to have almost reached its maximum value of around 40 mM. However as could be deduced from the curve describing the concentration of acetic acid, the anolyte is not near its stable state. Oxidation of acetic acid is a competing reaction, it is therefore expected that the ethanol oxidation rate will decrease with increasing concentration of acetic acid. This would lead to anodic ethanol concentrations exceeding the fitted top.

Taking both the uncertainty of the transport coefficient and the uncertainty of the anodic ethanol concentration into consideration, the following graph was constructed describing the loss of ethanol towards the anode relative to the production rate at 200 mA/cm^2 with an FE of 50% towards ethanol as a function of anodic concentration.

The uncertainty of the anodic ethanol concentration was addressed via extrapolation towards higher anodic concentrations. The uncertainty regarding the transport towards the anode was addressed via the application of different transport coefficients. The blue line signifies the loss at the transport coefficient determined under chronopotentiometric conditions, the red line is based upon the coefficient determined in the experiments without an applied potential. The red cross signifies the loss based on the fitted top of the anodic ethanol concentration as shown in Figure A.8 utilizing the calculated transport coefficient under potential.

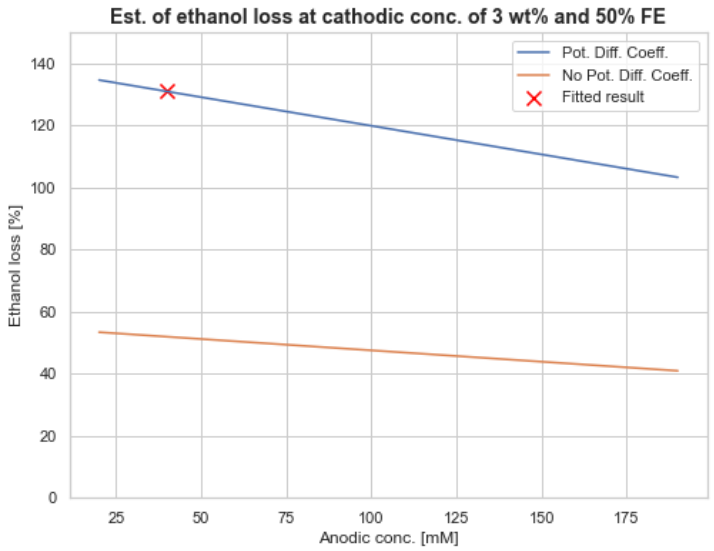

Figure A.9: Loss of ethanol relative to the production at 200 mA/cm^2 at a FE of 50% at various transport coefficients.

As can be deducted from Figure A.9, the hypothetical cell is estimated to be unable to sustain a 3 wt% cathodic concentration of ethanol. Utilizing the transport coefficient computed via the non-potential experiments a large improvement is found, however the losses are still in the same region as was reported for AEM based cells utilizing an MEA. Surprisingly, depending on the exact transport characteristics, ethanol crossover and subsequent oxidation might be a severe problem within the type of cells examined within this research.

A.3.3. Discussion

A number of limitations of these experiments are to be highlighted.

First of all a simple model based on Fick's law of diffusion was used to describe the ethanol crossover through the Nafion membrane. This assumption is an oversimplification as the electrolytes consist of at least three products.

Additionally an electro-osmotic drag coefficient of the form in Equation A.1 was neglected within these calculations [67].

$$J_{H_2O} = K_{drag} * J_{H^+} \tag{A.1}$$

The electro-osmotic drag coefficient K is proven hard to determine and no scientific consensus has been reached. Most values for a fully hydrated Nafion 117 membrane fall between 1 and 5 [28]. At a current density of 200 mA/cm^2 and electrolyte volumes of 50 ml, a simple calculation would yield a total water migration between 2 and 10 ml over the course of three hours, the electro-osmotic drag should therefore not be omitted. Table A.4 shows how the electro-osmotic drag coefficient could skewer the results compared to the assumption of an equal amount of catholyte and anolyte as was taken in calculations of the migration coefficient.

	Catholyte			**Anolyte**			**"Loss"**
	Vol. [ml]	Conc. [mM]	EtOH [mmol]	Vol. [ml]	Conc.	EtOH [mmol]	EtOH [mmol,%]
Assumed volumes	46,35	205.27	9,51	46,35	5,9	0.27	2.00 mmol, 17%
Potential volumes	56,35	205,27	11,57	36,35	5,9	0.21	

Table A.4: Potential apparent loss due to neglect of electro-osmotic drag

The potentially wrongfully assumed volumes along with the measured concentrations could cause a loss of over 17% of ethanol in case of the 0.25M tests, based on a 10 ml migration of water from anode to cathode. Note that this does not coincide with the losses as shown in Figure A.7 as it is known that acetic acid was produced in relatively large quantities, accounting for part of the loss of ethanol.

One effect worth mentioning, the osmotic pressure induced by increased phosphoric acid concentrations in the anolyte would counteract this water flux.

The migration of water due to EOD would lead to an overestimation of the transport coefficient as the cathodic concentration of ethanol would be observed to decrease while the anodic concentration follows the opposite path.

It should be noted that electro-osmotic drag is expected to have a minor effect on ethanol itself due to its size and neutrality, it primarily affects ethanol diffusion via the flux of water through the membrane. In the case of the cell designed, this water flux will reduce to zero, as the electrolyte is circulated indefinitely a stable state will arise and electro-osmotic drag will be counterbalanced by osmotic pressure.

A.3.4. Conclusion

It is clear that ethanol transport through a Nafion membrane will occur. To what extend is hard to determine based on the preliminary experiments as the electro-osmotic drag coefficient and the corresponding water flux were not taken into account. However the results suggest the loss of dozens of percentage points.

As ethanol extraction was crucial in the decision of cell design, crossover could have large implications on the validity of the design. Options to mitigate this potential problem lie on the substition of the 180 microns Nafion 117 membrane with a thicker or bipolar membrane.

A.3.5. Recommendations

It is clear that the electro-osmotic drag coefficient could not be omitted and that the experiment should be altered to incorporate this parameter. However as seen in Figure A.8, oxidation of ethanol is a significant factor, even in Nafion 117 based cells. The following adjustments on the test set-up are to be made:

1. A GC could be used to measure the CO2 content within the anodic gas output.
2. A properly calibrated HPLC should be used to enable determination of acetaldehyde concentrations at low quantities.
3. Inspired by the flooding tests, a scale could be used to measure the weight of catholyte and anolyte. Along with the ethanol concentrations via the HPLC and a density against ethanol concentration curve, the volumes of electrolyte could be computed. Assuming the influence of minor quantities of acetic acid and acetaldehyde on density of the mixture are negligible. Alternatively the amount of electrolyte could be measured after the test to estimate the need.

These alterations would enable the creation of a closed C-balance and provide deeper insight into the oxidation behaviour of ethanol. Furthermore via the computed volumes the influence of electro-osmotic drag coefficient could be estimated and accounted for in calculating the migration coefficient.

Using the described set-up it is believed that a more accurate picture could be drawn on the behaviour of ethanol at the relevant concentrations required for extraction, a vital step before commercialization.